

Qaanaaq 2001: mineral exploration in the Olrik Fjord – Kap Alexander region, North-West Greenland

Bjørn Thomassen, Johan D. Krebs and Peter R. Dawes



***Qaanaq 2001: mineral exploration in the
Olrik Fjord – Kap Alexander region,
North-West Greenland***

Bjørn Thomassen, Johan D. Krebs and Peter R. Dawes



Frontispiece. Geological discussion on the copper occurrence known as ‘Hill 620’ in the Mesoproterozoic Thule Supergroup. The persons are surrounded by malachite-stained, pale sandstones of the Qaanaaq Formation (Baffin Bay Group) with younger, darker, well-bedded clastic rocks of the Dundas Group in the background. The view is west along Olrik Fjord within the Olrik Fjord graben that juxtaposes the Precambrian shield (out of view left) and the Thule Supergroup. The summit of the sea-cliff in the background is 400 m above sea level. See also Figure 19.

Contents

1. Abstract	5
2. Introduction	6
3. Sample localities/numbers and place names	8
4. Geological setting	9
4.1 Precambrian shield.....	9
4.2 Thule Basin.....	10
4.3 Regional structures.....	11
5. Previous mineral exploration and known mineral occurrences	13
6. Remote sensing studies	15
6.1 Preprocessing.....	15
6.2 Processing.....	15
6.3 Geometric rectification.....	16
6.4 Anomalies.....	17
7. Mineral exploration in 2001	18
7.1 Thule mixed-gneiss complex.....	18
7.2 Smithson Bjerge magmatic association.....	21
7.3 Undifferentiated gneiss complex of Prudhoe Land.....	21
7.4 Prudhoe Land supracrustal complex.....	22
7.5 Nares Strait Group.....	23
7.6 Baffin Bay Group.....	24
7.7 Dundas Group.....	25
7.8 Regional structures.....	26
8. Conclusions and recommendations	27
9. Acknowledgments	29
10. References	30
Maps	
Map 1. Mineral reconnaissance projects	32
Map 2. Geological map of the Qaanaaq region	33
Map 3. Landsat anomaly map	34
Map 4. Sample locality and place name map (enclosure)	
Figures 1–22	35
G E U S	3

Tables

Table 1. Rock sample list	46
Table 2. Analytical results, rock samples	50
Table 3. Summary of selected elements	71
Table 4. Analytical values from the 'Mount Gyrfalco' showing	72

1. Abstract

Project *Qaanaaq 2001*, a one-season reconnaissance of the mineral potential and drainage geochemistry of the Olrik Fjord – Kap Alexander region, North-West Greenland, is a joint project of the Geological Survey of Denmark and Greenland and the Bureau of Minerals and Petroleum, Government of Greenland. This report covers the mineral potential part of the project.

A pre-season remote sensing study based on Landsat scenes pin-pointed 28 localities with mineralisation potential. The field work was ship-based and involved one period of helicopter support: it was mainly carried out as shoreline prospecting from rubber dinghy combined with traverses of active moraines and the check of known mineralisation and Landsat anomalies. The work was severely hampered by bad weather.

The project region comprises 4300 km² ice-free land underlain by Precambrian bedrock covered by Quaternary deposits. The bedrock is formed of two provinces: an Archaean–Palaeoproterozoic crystalline shield overlain by the unmetamorphosed Mesoproterozoic–?Neoproterozoic Thule Basin of sediments and volcanics (Thule Supergroup).

The crystalline shield displays widespread oxide and silicate facies banded iron-formation in the Archaean Thule mixed-gneiss complex suggesting a link to the major BIF province that stretches for 350 km along the coast of Melville Bugt and probably into northern Canada. Base metal mineralisation is also indicated and the geological environment invites further exploration for gold and base metals of sedimentary/exhalative origin.

The Palaeoproterozoic Prudhoe Land supracrustal complex hosts hydrothermally overprinted, pyrite-rich graphitic schists characterised by extensive colour anomalies registered as Landsat anomalies. Although no convincing signs of economic mineral concentrations were found, copper mineralisation is indicated and the rocks still constitute an interesting exploration target for reworked gold and base metals.

In the Thule Basin, red bed type copper mineralisation occurs both in the volcanic rocks of the Nares Strait Group and in fluvatile-continental sandstones of the Baffin Bay Group. The volcanic rocks also yield a number of geochemical gold anomalies and they are believed to have a potential for gold and copper.

A sequence of alternating stromatolitic limestone and black shale of the Dundas Group hosts minor sphalerite in the limestone and stratiform pyrite in the shale. These rocks extensively crop out south of the Qaanaaq region and they clearly warrant further exploration for base metals, especially since commercial lead-zinc concentrations exist in carbonate rocks of comparable age at Nanisivik in northern Canada.

Syn- to post-depositional faults of the Thule Basin may be mineralised with quartz, baryte and pyrite, and associated with red bed mineralisation.

2. Introduction

Qaanaaq 2001 is a one-season project aiming at assessing the mineral potential between Olrik Fjord and Kap Alexander (77°10'N – 78°10'N), North-West Greenland (Maps 1, 2). Similar projects were carried out in 1995, 1997 and 1998 in, respectively, Inglefield Land (78°10'–79°15'N; Thomassen & Dawes 1996), the Uummannaq district (70°30'–72°30'N; Steenfelt *et al.* 1998) and the Upernavik district (72°30'–75°30'N; Thomassen *et al.* 1999) (Map 1). The four projects, jointly run by the Geological Survey of Denmark and Greenland (GEUS) and the Bureau of Minerals and Petroleum (BMP), Government of Greenland, were mainly funded by the latter. The main goal of the initiative is to carry out basic mineral prospecting and stream sediment sampling in order to pin-point areas that could attract the interest of the mining industry. The 2001 field work comprised systematic drainage sampling, reconnaissance mineral exploration and geological studies.

The investigated region – herein referred to as the Qaanaaq region – comprises 4300 km² ice-free land centred on Qaanaaq, the administrative capital of Qaanaap (Thule) municipality. Much of the region is dominated by a 500–800 m high plateau capped by local ice caps and intersected by fjords and glaciers (Map 2). High dissected terrain occurs in Northumberland Ø and in the hinterland of Prudhoe Land where nunataks are common. The highest ice-free peak is c. 1000 m on Northumberland Ø. The climate is high arctic and the whole area is underlain by permafrost.

The field work was carried out between 22 July and 30 August by four geologists assisted by two young men from Qaanaaq (Thomassen 2001). The present authors had various tasks: B.Th. was mainly occupied with mineral exploration, J.D.K. had variable roles contributing both to the sediment sampling and the mineral exploration, as well as studying Landsat anomalies and P.R.D. consulted on the geology, collected new information and made map revisions. The fourth geologist was responsible for the geochemical sampling programme (Steenfelt *et al.* 2002) in which all other persons participated. A chartered 75-foot vessel, *M/S Kissavik*, served as a base, working from 12 anchorages (Figure 1). Two rubber dinghies enabled coastal work while the hinterland was reached by *Ecureuil AS 350* helicopter during a 14-day period (Figure 2). A field camp was established for three days on Northumberland Ø. The work was initiated in the north where the winter sea ice initially breaks up, then into Inglefield Bredning to reach the western islands and Olrik Fjord at the end of August. This ensured that reasonable ice conditions were encountered in all areas, apart from innermost Inglefield Bredning, north of Josephine Peary Ø, where thick calf ice rendered navigation impossible. For sixty per cent of the field period the work was seriously hampered by bad weather (rain and fog) with seven days totally lost.

The logistical and main geoscientific aspects of the project have been presented by, respectively, Thomassen (2001) and Thomassen *et al.* (2002). This report covers the mineral prospecting part of the project and presents brief field descriptions of the investigated mineral occurrences, as well as the locations and analytical results of the collected samples. Results from the stream sediment sampling part of the project have appeared in a separate report (Steenfelt *et al.* 2002); some of the geological observations made will be included in the ex-

planatory notes of the 1:500 000 geological map of the national map sheet coverage (Thule, sheet 5).

3. Sample localities/numbers and place names

The locations of the mineralised rock samples collected during *Qaanaaq 2001*, as well as all place names in the Qaanaaq region referred to in this report, are shown on Map 4. A selection of names, including all those outside the study region are shown on the other three maps.

The six-digit numbers starting with 4 (rock samples) or 5 (stream sediment samples) refer to samples collected during *Qaanaaq 2001* that officially have the prefix GGU and that are stored in the archives of the Geological Survey of Denmark and Greenland, Copenhagen. Other samples referred to are collected by the exploration company Nunaoil A/S (those prefixed Nunaoil) and as part of the Greenland mineral hunt programme *Ujarassiorit* that are identified by the letter U.

4. Geological setting

The Qaanaaq region is underlain by two bedrock provinces: a high-grade Archaean–Palaeoproterozoic crystalline shield overlain by unmetamorphosed Mesoproterozoic strata of the intracratonic Thule Basin (Figure 3). The profound unconformity between these two units is well preserved. The Thule Basin straddles Baffin Bay and the western outcrops are in coastal Ellesmere Island, Canada (Map 2). In Greenland, exposures form islands and the outer coastal areas bordered on the east by the shield.

The Qaanaaq region was mapped by the former Geological Survey of Greenland between 1971 and 1980, mainly by shoreline investigations with limited helicopter traversing inland. The western part exposing the Thule Basin has been mapped at 1:100 000; the area at the head of Inglefield Bredning, composed entirely of the Precambrian shield, is available at 1:200 000 (Dawes 1988). The only detailed mapping undertaken is of Smithson Bjerger (Nutman 1984). The Survey's 1:500 000 geological map sheet, Thule, sheet 5 (Dawes 1991) has a northern border at 78°N; the northernmost part of the project region around Kap Alexander is featured in Dawes (1997) and Dawes *et al.* (2000). Unless otherwise stated, rock unit names in this report are taken from the Survey's 1:500 000 map sheet.

4.1 Precambrian shield

Thule mixed-gneiss complex. This Archaean complex of highly deformed amphibolite- to granulite-facies gneisses forms the shield in the southern part of the study area (Map 2). It is composed of quartzo-feldspathic to pelitic paragneisses, multiphase orthogneisses with genetically related granitic rocks, as well as minor mafic and ultramafic bodies. The 2001 work confirmed that para- and multiphase orthogneisses are structurally complex and intricately associated on all scales. In many places the gneisses show pronounced compositional layering and the distinction of para- and orthogneisses can only be unravelled by detailed mapping. At the head of Inglefield Bredning pale garnet-bearing quartzitic layers associated with variable gneiss are conspicuous. At the head of Olrik Fjord, such rock associations contain a rusty unit of banded iron-formation (BIF), e.g. north-east of 'Mount Gyrfalco' (see later). In 2001, several previously mapped amphibolite bodies were found to grade into ultramafic rocks and new occurrences of ultramafic bodies were discovered, the largest being a boudin (c. 500 × 150 m) within orthogneiss at the head of Academy Bugt.

Smithson Bjerger magmatic association. This Archaean meta-igneous association is composed of the major Qaqujârssuaq anorthosite and various basic, dioritic and granitic intrusions, including the Heilprin Gletscher complex of Nutman (1984). The main anorthosite mass, seen in Figures 2 and 11, is predominantly anorthosite *sensu stricto* with minor leucogabbro, gabbro and ultramafic rocks. The rocks of the magmatic association that were intruded into the Thule mixed-gneiss complex have been affected by granulite facies metamorphism.

Undifferentiated gneiss complex. The gneisses of this unit are deemed to be mainly of Palaeoproterozoic age but it cannot be excluded that Archaean gneisses, corresponding to

those of the Thule mixed-gneiss complex, do occur. The unit contains the Prudhoe Land granulite complex of Dawes (1991; as named on the 1:500 000 map sheet), and the Etah Group, Etah meta-igneous complex and Palaeoproterozoic gneisses of Inglefield Land to the north (Map 2). In the study area, the main rocks are high-grade, polydeformed and polymetamorphosed orthogneisses with thin units of quartzo-feldspathic to pelitic paragneiss. The pelitic gneisses are commonly graphitic and they are made conspicuous by their rusty weathering. The paragneisses are considered to be correlatives of the larger tracts of supracrustal rocks that make up the next map unit.

Prudhoe Land supracrustal complex. These supracrustal rocks, of supposed Palaeoproterozoic age, comprise a thick succession of pelitic, semi-pelitic and quartzitic rocks (including pure quartz rocks) with some mafic units (amphibolite and pyroblastite) that form large, rusty-weathering outcrops in two main areas: around Morris Jesup Gletscher and to the east from Bowdoin Fjord to Josephine Peary Ø (Figure 4). In 2001, new outcrops of supracrustal rocks were noted in Bowdoin Fjord, between this fjord and McCormick Fjord and in Robertson Fjord. Units of marble, not hitherto known in the succession, were discovered at Bowdoin Fjord and Morris Jesup Gletscher. This strengthens the view that the supracrustal rocks are a correlative of the Etah Group of Inglefield Land in which marble is a conspicuous lithology (Dawes *et al.* 2000).

The supracrustal rocks have been folded by large recumbent isoclinal folds so that they now occur as shallow-dipping units that can be flanked both below and above by gneiss. The contacts examined between supracrustal rocks and the gneisses are tectonised but structural considerations suggest that the supracrustal rocks represent a cover sequence to the Thule mixed-gneiss complex (Figure 4).

4.2 Thule Basin

The Thule Basin developed on the peneplaned surface of the Precambrian shield (Figure 3). The basin fill – the Thule Supergroup – is a thick (possibly up to 8 km), multicoloured, continental, littoral to shallow marine sedimentary succession with one main interval of basaltic volcanic rocks that is seen on Figure 3. Basic sills are common at several levels. Five groups are recognised (Dawes 1997). The lower four groups are Mesoproterozoic in age (basal volcanics c. 1270 Ma). The upper strata (Narssârssuk Group) outcrop south of the study area; their age is uncertain thus explaining the Mesoproterozoic–?Neoproterozoic age assignment attributed to the Thule Supergroup. In Inglefield Land, north of the study area (Map 2), the Supergroup is overlain by Lower Palaeozoic deposits of the Franklinian Basin.

Smith Sound Group. This group directly overlies the crystalline shield; it represents the northern basin margin equivalent of the Nares Strait Group and the overlying Baffin Bay Group of the south. It is composed of varicoloured sandstones and shales, including red beds, with subordinate stromatolitic carbonates. No mineral prospecting of this group was carried out in 2001.

Nares Strait Group. This group, up to 1200 m thick and representing the oldest strata of the central basin, is dominated by sandstones (both red beds and clean white quartz arenites),

with one main interval of basaltic volcanics including flows, sills and volcanoclastic deposits (Cape Combermere Formation; Figure 3). Siltstone/shale- and carbonate-dominated intervals also occur. Stromatolites occur in the carbonates. The succession, that is divided into five formations, is taken to represent deposition in alluvial plain, littoral and offshore environments. In 2001, one important revision was made concerning the distribution of the group that has relevance to mineralisation. At Tikeraasaq the group was previously deemed absent where a postulated basement fault block was considered to be draped by the younger Baffin Bay Group (Dawes 1997). In 2001, a greenish basaltic unit, at least 20 m thick and in places veined and brecciated, was located within a red bed section directly overlying the crystalline shield: this succession is now referred to the Cape Combermere Formation. This formation has its maximum thickness in Greenland on Northumberland Ø (c. 200 m; reaches 340 m in Canada); it thins eastwards towards the basin margin petering out somewhere between Hubbard Gletscher and Kangerlussuaq.

Baffin Bay Group. This group represents the most widespread strata of the Thule Basin with a composite thickness of at least 1300 m. It is subdivided into five formations, four of which are present in Greenland. In the central part of the basin (western part of the study area) the group conformably overlies the Nares Strait Group; in the east it overlaps onto the crystalline shield. The group consists of shallow water, multicoloured siliciclastic rocks: sandstones, quartz grits and quartz-pebble conglomerates, with important intervals of shales and siltstones, representing mixed continental to marine shoreline environments, with syn-depositional faulting. The sandstones vary from highly ferruginous red beds to clean quartz sands. The uppermost strata (Qaanaaq Formation) indicate a gradually deepening depositional regime from predominantly alluvial plain to shallow-shelf, tide-dominated deposition that is part of a regional transgression of the shoreline that continues into the more basinal sequence of the Dundas Group.

The Dundas Group conformably overlies the previous group along a gradational contact. Its upper limit is marked by Quaternary deposits and the present erosion surface. The group has a dark weathering, monotonous lithology without conspicuous markers and regional correlation of sections is not obvious (Frontispiece, Figure 19); its estimated thickness is between 2000 and 3000 m. It is composed of sandstones, siltstones and shales with lesser amounts of carbonate and evaporite. Some carbonate beds have stromatolites and dark shales can contain stratiform pyrite. Deposition was in an overall deltaic to offshore environment. In the study area, two formations are recognised. In Prudhoe Land, the Kap Powell Formation is characterised by coarsening- and thickening-upwards shale–sandstone cycles thought to represent progradation delta front sequences, while the Olrik Fjord Formation, with a type section in the Olrik Fjord graben (Frontispiece), dominated by fissile, multicoloured shale packages with laminated silts and fine-grained sandstones is interpreted to represent prodelta muds and delta plain deposits. Sporadic basic sills are present; these are very conspicuous in the Dundas Group south of the study area.

4.3 Regional structures

The regional structure is dominated by the down-faulted blocks of Thule Supergroup forming islands and outer coastal areas bordered inland by generally higher elevation areas of the

Precambrian shield. Over much of its extent, the Thule Basin has preserved sedimentary contacts with the shield; in some places, for example in northern Prudhoe Land and in Olrik Fjord, faults delimit the basin deposits. Where the Dundas Group is downthrown against the shield, as in the Olrik Fjord graben (Map 2), displacement of several kilometres has taken place.

Compared to the gneisses and supracrustal rocks of the Precambrian shield, the Thule Supergroup is little disturbed. The main regional structures are fault blocks, grabens, large-scale flexures, as well as some local folds associated with faults. Prominent faults vary from NW–SE-trending, e.g. the fault blocks of Prudhoe Land, to WNW– ESE-trending as in the Olrik Fjord graben mentioned above. These latter faults are parallel to the most conspicuous basic dyke swarm of the region that is Neoproterozoic in age cutting all strata of the Thule Basin. In 2001, new faults of both trends were located. Of these, a steep fault at Scarlet Heart Gletscher (Map 2), has appreciable downthrow, juxtaposing the Baffin Bay Group against the gneisses of the shield.

5. Previous mineral exploration and known mineral occurrences

Limited mineral exploration has been carried out in the Qaanaaq region and no major mineral occurrences are known. In 1969, the commercial company Greenarctic Consortium discovered malachite-stained sandstone at a locality known as 'Hill 620' in Olrik Fjord during a reconnaissance survey (Stuart Smith & Campbell 1971; Map 2). In 1975 and 1977 the former Geological Survey of Greenland (GGU) investigated selected mineral occurrences found during regional mapping 1971–80 (Cooke 1978; Dawes 1991) and in 1978 banded iron-formation was recorded at Smithson Bjerger by Nutman (1984). Nunaoil A/S explored the Qaanaaq region in 1994 and 1995 and reported scattered malachite in the Thule Supergroup, as well as pyrite in a variety of settings (Gowen & Sheppard 1994; Gowen & Kelly 1996). Several mineralised rock samples from the Qaanaaq region collected by Greenlandic residents have been submitted to the Greenland mineral hunt programme, *Ujarassiorit* (Dunnells 1995, Olsen 2002). The main mineralised localities known prior to *Qaanaaq 2001* are listed below.

Olrik Fjord. The malachite mineralisation mentioned above at 'Hill 620' occurs in pale sandstones (Stuart Smith & Campbell 1971; Cooke 1978; Gowen & Sheppard 1994), now referred to the Qaanaaq Formation of the Baffin Bay Group (Frontispiece). Alteration and pyritisation occur in both Dundas Group sediments and in basement gneisses along the southern border fault of the Olrik Fjord graben (Gowen & Sheppard 1994). Two ultramafic pods (peridotite) in granitic gneiss south-east of Olrik Fjord host minor sulphide mineralisation. A sample of amphibolite with minor sulphides returned 116 ppm Au and 1204 ppm As (Gowen & Sheppard 1994).

Smithson Bjerger. Oxide and silicate facies iron-formations occur in paragneisses of this area (Nutman 1984). The maximum reported gold value is 33 ppb (Gowen & Sheppard 1994).

Bowdoin Fjord – Josephine Peary Ø. Within the supracrustal rocks of this area, semi-pelitic schists with up to 5% pyrite/pyrrhotite and magnetite, and in places highly altered and sheared, were reported by Gowen & Sheppard (1994) while Gowen & Kelly (1996) reported widespread alteration and pyritisation of paragneisses and amphibolites along faults and shear zones.

McCormick Fjord. Malachite staining on sandstones (now referred to the Qaanaaq Formation of the Baffin Bay Group) was observed at Red Cliffs by Gowen & Sheppard (1994). Widespread alteration and pyritisation of paragneisses and amphibolites along faults and shear zones were noted at Sun Gletscher (Gowen & Kelly 1996).

Robertson Fjord. The following *Ujarassiorit* samples stem from this area: a 2–3 cm large block of mainly chalcopyrite with >10% Cu, 0.27% Pb and 67 ppm Ag (U99-114) from 5 km north-east of Siorapaluk; vein quartz with chalcopyrite and 0.33% Cu from west of Siorapaluk (U01-313) and sand from Siorapaluk with 21% TiO₂, 61% Fe₂O₃ and 0.2% V (U93-849).

Northumberland Ø. Float of malachite-stained volcanic breccias (almost certainly derived from Cape Combermere Formation of the Nares Strait Group), malachite-stained sandstones and a grab sample of pyrite-bearing hornfels shale with 0.5 ppm Au and 3.8% Fe were reported by Gowen & Sheppard (1994) and Gowen & Kelly (1996). Malachite staining is also reported from the basal clastics of the Nares Strait Group on *Northumberland* Ø (Jackson 1986), as well as in the Cape Combermere Formation at Clarence Head, Ellesmere Island (Frisch & Christie 1982). Interesting *Ujarassiorit* samples include: *in situ* chalcopryrite with quartz and feldspar, > 10% Cu, 0.26% Pb, 49 ppm Ag and 1.5% Ba (U94-388), a boulder of massive sulphide with pyrite, sphalerite and calcite, and 7.1% Zn, 58.5% Fe₂O₃ and 6 ppm Hg, (U94-010, probably a fake sample from the Black Angel Mine, central West Greenland, i.e. within the frame marked Uummanaq on Map 1).

A total of 126 scattered stream sediment samples were collected in the present project area by Nunaoil 1994–95; these show modest metal concentrations viz. max. 56 ppb Au, 100 ppm Cu, 52 ppm Pb, 140 ppm Zn and 4400 ppm Ba (Gowen & Sheppard 1994; Gowen & Kelly 1996).

6. Remote sensing studies

An integral part of *Qaanaaq 2001* was a pre-season remote sensing study aimed at delineating areas of potential economic interest. It was based on four images of Landsat 7 ETM data recorded during the season of minimum snow cover (5 and 24 July 1999). The idea was to pin-point localities with mineralisation potential by means of mapping minerals that carry iron oxides (rust zones) and hydroxyl ions (clay alteration). Areas with coincident rust coloration and hydrothermal alteration are considered to have a potential for mineralisation.

A remote sensing study based on a Landsat 5 scene from 3 June 1991 was conducted by Nunaoil A/S in 1994. The scene was, however, of poor quality with heavy snow cover. No Fe-oxide alteration was detected whereas clay (hydroxyl) alteration was found to be widespread (Gowen & Sheppard 1994).

6.1 Preprocessing

Before actual treatment it was necessary to preprocess the data for the effects of surface cover, image defects, line dropouts, badly illuminated pixels, correction of sensor variation gain and offset. Five different types of surface characterise the study area: exposed bedrock, scree, fresh water lakes and streams, seawater, snow and ice. Since only the first two mentioned types are relevant to the study, the others were omitted before processing took place by the construction of masks. Areas in shadow were also omitted. As no ground truth was available for the construction of the masks, they were constructed using known biophysical properties and published spectral data. The spectral signature of the non-desired surface served as input for a box classification; it is characterised by its value in different bands, the bands that were used were dependent on the physical properties of the surface. The classification procedure had to be simple to ensure that it was applicable to all data sets with only minor adjustments though they were recorded at some temporal intervals. The contrast between noise and areas of interest was assumed to be large and therefore a simple procedure could be used without leading to unacceptable data loss. The band and DN (digital number) cut-off value used for the box classification were mostly determined from profiles across the feature/surface cover of interest.

6.2 Processing

Two different techniques were used for the processing of the data: (1) standard band ratios and (2) feature-oriented Principal Component Analysis.

(1) *Standard ratios*. The standard ratios maximise the lithologic information. This relation has been confirmed both empirically and physically. Crippen (1989) presented the arguments for the selection of the standard band ratios TM3/TM1 + TM4/TM5 and TM5/TM7 for the mapping of iron oxides and hydroxyl-carrying minerals, respectively. The selection of the bands contributing to the various ratios is based on transitions occurring in three compounds abundant in geologic material.

Iron oxides Fe-O. The Fe-O charge transfer transition occurs as a broad absorption band below 550 nm (Hunt 1977). This feature, situated in TM band 1 (blue-green) together with the high reflection in TM band 3 (red), is typical for iron oxide rusty colour (Hunt 1977). This will cause iron oxide stained areas to score high values in a TM3/TM1 ratio image.

Iron oxides Fe²⁺. Iron Fe²⁺ crystal field transitions for the ion in various forms of distorted octahedral sites with sixfold coordination occur as absorption bands in the region from 750–1500 nm (Hunt 1977). These features situated in TM band 4 (near infra red – NIR) can be used to detect iron oxides using the TM4/TM5 as most minerals reflect well in TM band 5 (short wave infra red – SWIR). This ratio will score high and low values depending on whether these oxides are present or not. The iron in augite will also be detected by this ratio; however, this is of limited importance as iron oxide surface coating will cloak this weak contribution.

Hydroxyl OH⁻. Hydroxyl OH⁻ has only one fundamental stretching mode located near 2750 nm with the exact location depending on what the group is directly attached to and the site it occupies. These features fall outside the spectral capability of the Landsat TM. However, the overtones all lie in the 2200–2400 nm range well within TM7 (SWIR). Using the fact that most minerals reflect well in TM band 5 (SWIR), the ratio TM5/TM7 will score high values where hydroxyl-bearing minerals are present.

(2) *Feature-oriented Principal Component Analysis (PCA)*. This process is also called the Crosta technique after its originator (Crosta & McMoore 1989). It bears a slight resemblance to the band ratio technique. The band selection process is the same as the one used for the standard ratio technique TM3 vs. TM1 and TM4 vs. TM5 for the mapping of iron oxides, and TM5 vs. TM7 for hydroxyl mapping. The idea is again to find areas where a high reflection in TM5, linked with a low reflection in TM4, indicate the presence of Fe-O, areas where high reflection in TM5, linked with a low reflection in TM1, indicate the presence of Fe²⁺, and areas where high reflection in TM5, linked with a low reflection in TM7, indicate the presence of hydroxyl. The aim is to select the input bands to the PCA in such a way that areas where the above is fulfilled will appear as abnormal values. As input 2, combinations of four bands each, are used TM1, TM3, TM4 and TM5 for the mapping of iron oxides, and TM1, TM3, TM5 and TM7 for hydroxyl mapping (Loughlin 1991a). The reason for only conducting PCA on four bands instead of all six is to assure that certain materials will not be mapped, and to increase the likelihood that others will be unequivocally mapped into only one of the PC images (Loughlin 1991b). To locate where the information of the different input TM bands goes, the values of the eigenvector loading for the input bands is needed. This loading is directly read from the eigenvalue matrix. By combining these three data sets in a RGB (red, green, blue) display as hydroxyl, iron and hydroxyl + iron, areas with hydrothermal alteration will be red, those with iron oxide staining green, and areas with both, bright white. This image is called the Crosta image.

6.3 Geometric rectification

The Landsat data of the study area were rectified using a second-order model with Ground Control points supplied by T. Tukiainen (GEUS). The produced image data were reproduced

in paper copies consisting of one Crosta map at 1:250 000 and four Crosta maps, NW, NE, SW, SE, at 1:100 000, and in the UTM projection. The maps were also placed on the project's laptop computer and co-registered with a digital geological map over the study area, to make cross referencing possible.

6.4 Anomalies

An anomaly was defined as a pixel where both processing techniques gave a digital number (DN) above 253 (corresponding to 0.0008% of the data), in both the Fe and the OH⁻ images, providing it had a minimum of two pixels with similar values as neighbours. Using this, 28 anomalies were registered in the following rock units: Thule mixed-gneiss complex (two), Prudhoe Land supracrustal complex (eleven), Baffin Bay Group (four) and Dundas Group (eleven) (Map 3).

A rough distinction between the major lithological units is apparent in the image data with the Dundas Group showing up as being iron oxide stained. Unfortunately, this meant that small erosional windows or isolated exposures of the Dundas Group were registered as anomalies that proved of little interest from a prospecting viewpoint. Previously known zones of alteration and rust colouring were all represented by anomalies in the image data and most of these were visited, as for example the rusty supracrustal rocks north of Inglefield Bredning (Figures 4, 13). It became apparent that the statistical criteria selected had too high cut-off values as several exploration targets encountered during the season were visible in the image data, but *not* registered as being abnormal. It transpires that a reduction of the selected DN cut-off value from 253 to 252 would have resulted in 306 anomalies. All areas of alteration and/or rust coloration observed in the field were registered in the processed Landsat data.

7. Mineral exploration in 2001

We aimed at a systematic visual inspection for signs of mineralisation along the entire coast of the Qaanaaq region but this was partially thwarted by miserable weather. The work was carried out partly as shoreline prospecting – observations from a rubber dinghy sailing slowly along the coast, combined with onshore investigations of promising localities – and partly as traversing of lateral and terminal moraines of active glaciers for mineralised blocks stemming from hinterland mountains. This work was supplemented by limited helicopter-supported checks of inland localities. In addition to this work, special attention was paid to anomalies detected on the Landsat images, previously known mineral indications, *Ujarassiorit* localities, and promising lithologies and structures, as outlined by Thomassen & Krebs (2001). Since previous work had concentrated on the Thule Supergroup, the main emphasis of the 2001 field work was on the various lithologies of the Precambrian shield.

A total of 152 mineralised rock samples were collected. These were mainly loose blocks from moraines, stream beds and scree (126) but also chip and grab samples from outcrop (26). They are briefly described in Table 1 with GPS geographical co-ordinates and plotted on Map 4. All samples have been analysed for 49 elements by a combination of instrumental neutron activation and inductively coupled plasma emission spectrometry at Activation Laboratories Ltd., Ontario, Canada. Additionally, 40 of the samples yielding elevated gold values or other interesting features, were assayed for gold, platinum and palladium by fire-assay methods. All analytical results are presented in Table 2 and a chemical summary is given in Table 3.

In the following, activities and results from the investigated areas are described and commented on, cf. Map 4. The description is based on field observations and analytical results supplemented by some preliminary microscope observations in reflected light.

7.1 Thule mixed-gneiss complex

Work carried out

Shoreline prospecting was carried out at Kap Trautwine, innermost Olrik Fjord, Tikeraasaq, Academy Bugt, western Smithson Bjerger and south-west of Qattarsuit. Active moraines were traversed in northern Steensby Land (Misuumasoq, Politiken Bræ and Savage Gletscher), Hubbard Gletscher and Bowdoin Gletscher. Helicopter stops were made at 'Mount Gyrfalco', south-east of Academy Bugt and central Smithson Bjerger.

Results

At Kap Trautwine, abundant scree blocks of oxide facies banded iron-formation (BIF) with minor disseminated iron sulphides were observed (Figures 5, 6; 485815, 19–21). Scree blocks of gneiss and amphibolite with disseminated iron sulphides were also collected (485811–14, 16, 17, 22).

The moraines of the glaciers of northern Steensby Land yielded a number of gneiss and ultramafite–amphibolite blocks with pyrrhotite and minor chalcopyrite, and up to 37 ppb Au, 1748 ppm Cu and 1289 ppm Ni (470029, 485805–10, 23–29).

North-east of 'Mount Gyrfalco', a rust zone registered as a Landsat anomaly turned out to be associated with a c. 20 m thick unit of oxide facies BIF with a strike length of c. 500 m (485729–34). To the west, the unit ends in the east wall of a major valley, and to the east it is involved in a tight fold closure (Figures 7, 8). It comprises cm-scale interbedded quartz, magnetite, pyroxene and garnet with minor iron sulphides (Figures 9, 10). Semi-quantitative XRD analyses performed by Activation Laboratories on two samples (485729 and 485731) show 45–70% quartz, 15–30% orthoferrosilite (Fe, Mg)SiO₃ and 15–30% magnetite. Chip samples over 6.5 m returned 30.5% Fe, 2.1% Mn, 0.8% S and 8 ppb Au. Selected analytical values are shown in Table 4. In addition to iron, the samples have relatively high concentrations of manganese, sulphur and zinc.

In inner Olrik Fjord, two 100 x 500 m bodies of amphibolite and ultramafic rocks, observed from the sea, showed no sign of malachite staining. A small mafic complex on the south coast of the fjord yielded blocks with pyrrhotite and up to 31 ppb Au, 1047 ppm Cu, 1297 ppm Ni and 2850 ppm Cr (485801–03). Blocks of mafic–ultramafic rocks with pyrite (485798–485800) and garnet quartzite with minor iron sulphides (485797) were collected in some of the deltas.

South-east of Academy Bugt, a 150 x 500 m mafic–ultramafic body showed faint malachite-staining but the collected grab sample returned only 261 ppm Cu (485735). At the shore, a quartz vein, a few centimetres thick, with trace sulphides, was observed in an ultramafic lens (485739).

At Smithson Bjerge, blocks of often irregular cm-banded quartz-garnet-pyroxene-hornblende rocks were collected in the deltas of the two main streams (485741–47). They contain disseminated pyrrhotite, magnetite and graphite, minor chalcopyrite and traces of arsenopyrite, with up to 83 ppb Au. In central Smithson Bjerge blocks of similar rocks, and more magnetite-rich rocks were collected (Figure 11; 470020, 485722–25).

South-west of Qattarsuit, faint malachite staining was observed over a distance of 3–4 km in steep coastal cliffs of banded gneisses (Figure 12). Samples of melanocratic paragneiss collected at one locality (485748–50) host minor disseminated pyrite and chalcopyrite, the latter partly remobilised into veinlets. Such mineralisation could explain the malachite staining. The samples returned no significant metal values (max. 10 ppb Au and 213 ppm Cu). Scree blocks of garnet quartzite with pyrrhotite, minor magnetite and traces of chalcopyrite were also collected at this locality (485751–54).

Hubbard Gletscher moraines were found to be especially enriched in BIF blocks with traces of iron sulphides (470022, 485766, 69, 71) and garnet quartzite/paragneiss with pyrite and up to 931 ppm Cu and 3282 ppm Ni (470021, 23; 485768, 70).

Bowdoin Gletscher yielded blocks of mostly garnet quartzite/paragneiss with iron sulphides (485755, 56, 58, 59).

Comments

The mineralisation in the Thule mixed-gneiss complex can be grouped in the following way:

(1) Oxide facies iron-formation. Magnetite, often in the form of iron-formation, is common in paragneiss blocks wherever the Thule mixed-gneiss complex forms the bedrock. The magnetite-bearing samples represent a number of lithologies varying from mm- to cm-scale interbedded magnetite, silicates and quartz rocks, i.e. oxide facies banded iron-formation (BIF; Figures 9, 10), to near massive magnetite-silicate rocks without any obvious macrostructure. Analyses of 17 magnetite-rich samples show the following median values, with maximum values in brackets: Fe: 27.8 (35.6)%, Mn: 1677 (28051) ppm, Ti: 0.05 (0.51)%, P: 0.08 (0.12)%, V: 20 (120) ppm, Cu: 37 (300) ppm, Zn: 75 (361) ppm, S: 0.34 (2.53)% and Au: < 2 (19) ppb. The chemistry confirms the assumption that the rocks are of sedimentary, rather than magmatic, origin (low Ti, V and P).

The magnetite occurrences found in 2001 can be interpreted as the northward extension of the Archaean magnetite province that stretches for 350 km along the coast of Melville Bugt and into the Pituffik (Thule Air Base) area (Dawes 1976, 1991; Dawes & Frisch 1981). This province is a prime candidate for correlation with the Algoma-type iron deposits of the Mary River Group of northern Baffin Island (Jackson 2000). In addition to iron, BIF provinces have a potential for gold and base metals.

(2) Silicate facies iron-formation. Blocks of often banded quartz-garnet (-pyroxene-amphibole) rocks with disseminated pyrrhotite, magnetite and traces of chalcopyrite were encountered at several localities in the eastern part of the region. Similar rocks of ferruginous quartzite “perhaps akin to silicate facies banded iron formation” were described from Smithson Bjerger by Nutman (1984, p. 9). Analyses of 24 samples show the following median values, with maximum values in brackets: Fe: 14.3 (26.9)%, Mn: 866 (4344) ppm, Cu: 126 (1089) ppm, Zn: 89 (793) ppm, S: 1.6 (4.4)% and Au: 4 (83) ppb. Most of the samples collected by us on Smithson Bjerger (470020, 485722, 24, 41–47) and south-west of Qattarsuit (485751–54) contain 20–25% Fe and are regarded as silicate facies iron-formation whereas samples from other areas yield lower iron concentrations. These two areas are also depicted as base metal anomalies in the geochemical survey (Steenfelt *et al.* 2002). In general, the quartz-garnet rich rocks are regarded as being derived from chemical sediments or exhalites and to have good mineralisation potential.

(3) Copper-bearing paragneiss. Copper mineralisation possibly hosted by melanocratic paragneiss may be widespread in the cliffs south-west of Qattarsuit. This coast also figures as a multi-element anomaly (Ni, Zn, Pb, Cu) in the stream-sediment analyses, indicating a potential for sediment-hosted base metal mineralisation (Steenfelt *et al.* 2002).

(4) Copper-bearing magmatic rocks. Faint malachite coatings, caused by minor disseminated chalcopyrite, occur on amphibolitic and ultramafic lenses and pods in the gneisses. Analyses of 17 samples show the following median values, with maximum values in brackets: Fe: 11.3 (20.0)%, Mn: 2182 (7039) ppm, Ti: 0.55 (1.72)%, Cu: 383 (1748) ppm, Ni: 176 (1297) ppm, Co: 105 (239) ppm, Cr: 141 (2850) ppm, S: 1.21 (8.21)%, Au: < 2 (31) ppb, Pt: <5 (8) ppb

and Pd: < 4 (19) ppb. It is concluded, that no significant magmatic metal concentrations have been found to date.

(5) Sulphide-bearing shear zones. A number of blocks of high-strain rocks with minor disseminated iron sulphides, believed to stem from shear zones, were collected at various localities. However, gold was not detected in these samples (485740, 57, 74, 78).

7.2 Smithson Bjerge magmatic association

Apart from brief shoreline prospecting of the promontory north-west of Heilprin Gletscher, these rocks were not investigated by us. There was no sign of mineralisation in the gabbroic rocks of this locality.

7.3 Undifferentiated gneiss complex of Prudhoe Land

Work carried out

Investigations along the Prudhoe Land coast between McCormick Fjord and Kap Alexander were hampered by the lack of rubber boats at the start of the field work; thus investigations were restricted to the moraines of Bamse Gletscher, Clement Markham Gletscher, the snout of Morris Jesup Gletscher, Meehan Gletscher and Sun Gletscher, supplemented with shoreline prospecting in parts of Robertson Fjord and McCormick Fjord.

Results

At Bamse Gletscher and Clement Markham Gletscher, the moraines yielded a number of rusty blocks of paragneiss and garnet quartzite with disseminated graphite, pyrrhotite and traces of chalcopyrite with up to 76 ppb Au (470001, 03–08; 485701–06).

At Morris Jesup Gletscher, active moraines are not accessible from the coast. Older moraines yielded blocks of marble with trace chalcopyrite (probably from the Prudhoe Land supracrustal complex – 485707), and a pegmatite boulder with massive, coarse graphite which returned 1213 ppm Mo (485708).

Innermost Robertson Fjord and Meehan Gletscher yielded amphibolites with minor sulphides (485779, 80), and garnet quartzite with pyrrhotite and up to 62 ppb Au (470026, 485781, 82).

At Sun Gletscher, a rusty horizon, c. 10 m thick, was observed on the west side, 100–200 m above the glacier. Blocks stemming from this horizon consist of graphitic garnet quartzite without sulphides.

Comments

A number of rusty moraine blocks of paragneiss, siliceous gneiss, garnet quartzite and amphibolite derived from this unit contain disseminated iron sulphides, graphite and traces of chalcopyrite. Some samples are slightly enriched in gold and base metals (Table 3) but no significant finds were made.

7.4 Prudhoe Land supracrustal complex

Work carried out

Shoreline prospecting was done on the east side of Bowdoin Fjord including traversing up to Gable Gletscher and at Qattarsuit. Helicopter-supported investigations were made at Sugarloaf and north of Morris Jesup Gletscher.

Results

At Gable Gletscher, the western part of a distinct colour anomaly was traversed and a pyritic graphite schist unit more than 10 m thick was investigated and sampled (Figure 13; 485761–65). The very crumbly schist may contain 10–20% graphite and 5–15% conformable pyrite and is ‘bound together’ by mm–cm thick layers and lenses of pyrite-bearing quartz and quartz-feldspar neosome (Figure 14). The pyrite forms veinlets and meshes in the neosome indicating remobilisation caused by a hydrothermal overprint, which is also indicated by the widespread clay alteration (Figure 15). Metal concentrations are low, max. 6 ppb Au, 213 ppm Cu, 135 ppm Pb, 160 ppm Zn, 581 ppm Ni and 116 ppm Mo.

On the east coast of Bowdoin Fjord, a canary yellow spot at 200 m a.s.l. was inspected in dense fog. It consists of yellow clay, formed by alteration of the local pyritic graphite schist, which causes yellow coloration of the local stream. Grab samples of graphite schist with pyrite (Figure 16; 485772) and sub-outcrops of amphibolite with pyrite (485773) returned up to 11 ppb Au, 166 ppm Cu, 637 ppm Zn and 40 ppm Mo.

At Sugarloaf, an outlier of orthogneiss rests on quartzite and a more than 100 m thick sequence of graphitic and pyritic garnet schist. The schist hosts frequent neosome quartz-feldspar layers and lenses with pyrite on hairline fractures (485721). Widespread clay alteration of the schist causes vivid red and yellow coloration. A chip sample collected over 1 m of graphitic-pyritic mica schist returned no significant metal values (485720).

At Qattarsuit, red coloration of the supracrustal rocks is widespread, but no sulphide mineralisation was observed by us during brief shoreline prospecting.

At a nunatak north of Morris Jesup Gletscher, a 300–400 m thick section of rusty, graphite-bearing mica schists with intercalations of amphibolite, quartzite and marble was traversed. Faint malachite staining was observed on a few metres thick layer of a garnet-rich mafic rock with minor disseminated magnetite, pyrrhotite and chalcopyrite. A grab sample returned 886 ppm Cu and 3.1% Ti (485715). At the top of the section, a c. 50 m thick unit of white, glassy quartzite with thin, isoclinally folded pelite bands occurs. At the basal 0.5 m of this bed, faint malachite staining caused by scattered, few mm-large blebs of chalcopyrite occur for more than 150 m laterally (Figure 17). A grab sample returned 183 ppm Cu and 46 ppm W (485716).

Comments

In the east, this map unit is characterised by conspicuous red and yellow rust zones in sulphiditic semi-pelitic schist and these correspond to concentrations of Landsat anomalies (Map 3). Checks at three localities east of Bowdoin Fjord revealed units of highly graphitic and pyritic schist several tens of metres thick with intense clay alteration; remobilisation of

pyrite into veinlets in quartz-rich pinch-and swell layers is interpreted as due to hydrothermal overprinting. Analyses of chip and grab samples show no significant concentrations of economic metals (Table 3). Maximum values of nine samples are: 11 ppb Au, 213 ppm Cu, 135 ppm Pb, 637 ppm Zn, 116 ppm Mo, 581 ppm Ni, 151 ppm Co, 16.6% Fe, 18.21% S, 20 ppm Se, 9.3 ppm U and 15 ppm W. Although these figures are not encouraging, the vast amount of iron sulphide and the widespread alteration in the area invites further exploration for re-worked or epigenetic metal concentrations. Furthermore, the stream-sediment geochemistry suggests the presence of metasedimentary units with concentrations of REE-rich minerals (Steenfelt *et al.* 2002).

An interesting result of the Landsat study is the presence of rust zones in the Prudhoe Land supracrustal complex and their paucity in other shield lithologies. In Inglefield Land to the north (Map 2), rust zones caused by iron sulphides and graphite are also concentrated in supracrustal rocks of the Etah Group and derived paragneisses (Dawes *et al.* 2000; Thomassen *et al.* 2000). This supports our view that the Prudhoe Land supracrustal complex is a correlative of the Etah Group, and thus could host a similar potential for copper-gold mineralisation.

To the west, at Morris Jesup Gletscher, highly pyritic units were not observed and hydrothermal alteration is not evident, but minor copper mineralisation occurs in quartzite. Thus, it is interesting that two copper-bearing *Ujarassiorit* floats have been collected 7–8 km south of Morris Jesup Gletscher: glassy, bluish quartzite with mm-size blebs of chalcopyrite and 0.33% Cu from west of Siorapaluk (U01-313), and a small piece of chalcopyrite from north-east of Siorapaluk (U99-114). These are regarded as stemming from quartzite of the Prudhoe Land supracrustals and indicate that quartzite-hosted copper mineralisation is widespread in this area. The host rock seems to be a true quartzite, derived from clean beach sands.

7.5 Nares Strait Group

Work carried out

Volcanic rocks from the Cape Combermere Formation of this Group were inspected during shoreline prospecting in McCormick Fjord, in the moraines of Bamse Gletscher, Semiarsusuaq and the glacier east of Robins Gletscher, and during traversing at Tikeraasaq.

Results

Mineralisation was only noted in moraine blocks on the glacier east of Robins Gletscher on Northumberland Ø. Here malachite occurs as coatings and blebs on various volcanic rocks. The moraine stems from the steep mountain immediately south of the glacier, where rocks of the Cape Combermere Formation are in fault contact with the Baffin Bay Group along the NW–SE-trending Kiatak Fault, a major dislocation juxtaposing the Dundas and Nares Strait Groups (Dawes 1997, p. 60). The following rock types were collected: carbonate-cemented volcanic breccia with hematite needles (485792, 93), vesicular agglomerate with malachite and 1362 ppm Cu (485794), volcanic agglomerate with malachite, covellite and digenite, and 1.02% Cu, 11 ppm Ag and 0.86% Ba (Figure 18; 485795) and homogenous basalt with malachite coating and 479 ppm Cu (485796). A solitaire, walnut sized, 'high grade' mala-

chite-hematite fragment was also analysed (485791). It returned > 10% Cu, 0.2% Pb, 96 ppb Au, 156 ppm Ag, 44 ppb Pt, 127 ppb Pd, 31.9% Fe, 0.43% S and 1.4% Ba.

Comments

The copper mineralisation in the Cape Combermere Formation resembles a 'volcanic red bed copper' deposit type (Kirkham 1996), possibly associated with the NW–SE-trending Kiatak Fault that crosses Northumberland Ø.

It should be noted that the highest gold concentrations recorded in the geochemical surveys carried out by Nunaoil A/S 1994–95 and by us in 2001 stem from streams draining this Group (Gowen & Sheppard 1994; Gowen & Kelly 1996; Steenfelt *et al.* 2002). The anomalous stream sediment samples are listed below:

- Northern Northumberland Ø: 38 ppb Au (GGU 506118), 14 ppb Au (Nunaoil 193553) and 8 ppb Au (Nunaoil 193554).
- Bowdoin Fjord east: 24 ppb Au (Nunaoil 193582), 8 ppb Au (Nunaoil 193580).
- West of Hubbard Gletscher: 55 ppb Au (GGU 506140).
- Near the former Kangerlussuaq settlement, Inglefield Bredning, where the Group is believed to occur: 56 ppb Au (Nunaoil 193594), 17 ppb Au (GGU 506089).

It is not known, if there is connection between the copper mineralised volcanics and the gold anomalies but the rift volcanicity of the Cape Combermere Formation would be a favourable environment also for gold mineralisation. Neither is it known whether the pyritic hornfels shale with 0.5 ppm Au reported from northern Northumberland Ø stems from this Group or from the overlying Dundas Group (Nunaoil 109455; Gowen & Kelly 1996). The same applies to the copper-rich *Ujarassiorit* sample collected on the eastern part of the island (U94–388). In spite of these uncertainties, the volcanic unit emerges as a promising target for gold-copper exploration.

7.6 Baffin Bay Group

Work carried out

Shoreline prospecting was conducted on the south shore of Olrik Fjord, south-east of Qaanaaq and in McCormick Fjord. Moraines were checked on Semiarsussuaq and a helicopter stop was made at 'Hill 620'.

Results

'Hill 620' was initially visited during a brief helicopter stop (Frontispiece, Figure 19); closer investigation during shoreline prospecting was thwarted by thick fog and rain. The showing comprises an isolated, 100 × 100 m area, adjacent to an E–W-striking fault and covered by cm-dm sized blocks of malachite-sprinkled white sandstone of the Qaanaaq Formation (485726). Faint malachite staining was also observed on sandstones 100–200 m farther to the south-west. Under the microscope rare, up to 50 µ large interstitial grains of chalcopyrite, pyrite, and occasionally bornite-digenite-covellite, were seen. A composite grab sample returned 0.4% Cu, 5 ppm Ag and 0.3% Ba.

In low coastal exposures south-east of Qaanaaq, interbedded sandstone and shale of the Qaanaaq Formation display very faint malachite staining. Composite samples were collected from 5 cm pale sandstone with malachite (485830) and 10 cm black shale on top of this (485831). The sandstone contains scattered, small interstitial grains of chalcopyrite and subordinate pyrite and returned 1116 ppm Cu, whereas the shale gave 119 ppm Cu only.

Red Cliffs in McCormick Fjord own their name to oxidised sandstones of the Baffin Bay Group. Minor pyrite-copper mineralisation was observed in sandstones of the Qaanaaq Formation below these red beds: some 20 m above sea level, faint malachite staining occurs on white sandstone with scattered, 0.5 cm-size specks of pyrite. A selected composite sample returned only 7 ppm Cu (485711). 200 m further east and stratigraphically lower, a small outcrop in the scree near sea level showed faint malachite staining (Figure 20). It comprises dm-thick layers of interbedded pale sandstone and black shales. Specks of chalcopyrite were observed in the sandstone, and a selected composite sample returned 1.5% Cu (485712). Under the microscope interstitial chalcopyrite and traces of pyrite were seen. A scree block of white, conglomeratic sandstone with concretionary pyrite and 0.8% Ba was collected nearby (485713), and a similar block was collected at the coast south of Red Cliffs (470030).

On the north-west coast of McCormick Fjord, a local block of pale sandstone with malachite coating and minor disseminated chalcopyrite and pyrite returned 358 ppm Cu (485714).

The moraines of Semiarsussuaq glacier on Northumberland Ø contain many blocks of rusty sandstone with minor disseminated pyrite and occasionally malachite and chalcopyrite with up to 665 ppm Cu (485783, 84).

Comments

Faint malachite staining on pale sandstones was observed at several localities in the Qaanaaq Formation of the Baffin Bay Group. This is caused by oxidation of minor chalcopyrite and pyrite as flecks and disseminations. This red bed type mineralisation is probably of diagenetic origin, perhaps controlled by local faults. The copper concentrations encountered until now are very modest.

7.7 Dundas Group

Work carried out

Limited shoreline prospecting was accomplished at Kap Chalon, the moraines of Clement Markham Gletscher and Savage Gletscher were checked, and some traversing was done on north-eastern Northumberland Ø.

Results

At Savage Gletscher, minor irregularly disseminated pyrite was observed in moraine blocks of white sandstone. A pyrite-rich sample returned nothing of interest (485804).

At Kap Chalon and Clement Markham Gletscher, widely scattered, mm-sized spots of pyrite occur in sandstone. A moraine boulder shows no noticeable metal concentrations (470002).

On Northumberland Ø, the Group shows various signs of mineralisation. As noted by Dawes (1997), stratiform pyrite is at some levels common in sandy shales of the Dundas Group (particularly the Steensby Land Formation). Such mineralisation is common on the north-eastern part of the island, but no significant base metal concentrations were recorded by us. The collected grab samples returned max. 212 ppm Cu, 48 ppm Pb and 214 ppm Zn (470027, 485785, 485787–89). Two samples of brecciated black shale with diastasis cracks cemented by white calcite with a few specks of chalcopyrite returned up to 426 ppm Cu, 157 ppm Pb and 461 ppm Zn (470028, 485790). In a sequence of interbedded shale and stromatolitic limestone, minor sphalerite was observed at the base of a limestone unit (Figure 21). A composite sample returned 2.1% Zn and 0.01% Pb (485786). Also of interest here is the observation by Marcos Zentilli (personal communication 2002) in the same area of minor galena-baryte mineralisation at a basic sill / shale contact.

Comments

The find of sphalerite in stromatolitic limestone encourages to further exploration for base metals, and it is worth noting that extensive outcrops of the Group (Steensby Land Formation) occur south of the Qaanaaq region.

7.8 Regional structures

Work carried out

The border faults of the Thule Basin were checked by a helicopter fly past along the south coast of Olrik Fjord, by traversing in the moraines of Savage Gletscher and at Tikeraasaq and inspected during shoreline prospecting in Robertson Fjord and McCormick Fjord.

Results

Yellow clay alteration, as recorded in the Landsat study, was observed from the air along the southern fault of the Olrik Fjord graben. *In situ* mineralisation was found only at one locality, c. 3 km east of Savage Gletscher. Here brecciated and hydrothermally altered gneiss in the fault zone hosts a mesh of quartz veins and veinlets with pyrite and marcasite. Two composite samples collected with a lateral distance of 1 m in the crumbling and poorly exposed fault zone returned no noticeable metal concentrations, apart from 5500 ppm Ba (485727, 28).

At Tikeraasaq, a system of NW-trending, 0.5 cm thick quartz veins with traces of chalcopyrite was observed in the gneiss of the main stream bed (Figure 22; 485718). A composite sample returned 217 ppm Cu and 26 ppm W. A block of siliceous breccia with traces of chalcopyrite gave 1068 ppm Cu (485717).

Comments

The syn- to post-depositional faults of the Thule Basin seem to be mineralised with quartz, baryte and pyrite +/- chalcopyrite, an observation supported by the stream-sediment geochemistry (Steenfelt *et al.* 2002). It is noteworthy that the highest barium concentrations in stream sediments from both the Nunaoil survey and the GEUS survey stem from the south-east end of the Kiataq Fault on Northumberland Ø: 4400 ppm Ba (Nunaoil 193557) and 5400 ppm Ba (GGU 506126).

8. Conclusions and recommendations

The pre-season Landsat study successfully outlined 28 anomalies as targets for field checks and thus gave a first impression of the regional distribution of rust zones and hydrothermal alteration. A striking result is the presence of rust zones in the Prudhoe Land supracrustal complex and their paucity in the other shield lithologies. The field work showed 17 of the anomalies to be related to mineralisation and/or hydrothermal alteration, the remainder stemming from formational responses. Therefore, it is recommended to apply this method in future reconnaissance projects.

The widespread occurrence of banded iron-formations in the Thule mixed-gneiss complex links the Qaanaaq region up with the major Archaean BIF province that stretches for 350 km along the coast of Melville Bugt and into the Pituffik area, and probably continues to the south-west on Baffin Island in northern Canada. Although no significant metal concentrations other than iron were encountered in these rocks during the present study, base metal mineralisation is indicated, and the geological environment invites further exploration for gold and base metals of sedimentary/exhalative origin. Obvious targets are the mixed gneisses in the cliffs south-west of Qattarsuit with their malachite staining and multi-element geochemical anomaly, as well as the anomalous paragneisses of southern Smithson Bjerge.

The undifferentiated gneiss complex of Prudhoe Land yielded a number of mineralised moraine blocks of paragneiss with slightly enhanced gold and base metal concentrations. However, no obvious indications of significant mineralisation were detected by us and no further exploration of this unit is recommended.

Although no convincing signs of economic mineral concentrations were found in the hydrothermally overprinted, pyrite-rich graphitic schists of the Prudhoe Land supracrustal complex, the unit constitutes an obvious exploration target and needs much closer scrutiny to verify whether it has a real potential for reworked gold and base metals. Copper mineralisation is indicated in western outcrops of this unit.

The red bed copper mineralisation in the volcanic rocks of the Nares Strait Group is possibly associated with the NW–SE-trending, barium-anomalous Kiatak Fault crossing Northumberland Ø. A gold potential is also indicated by the drainage geochemistry, and this volcanic unit (Cape Combermere Formation) and the faults crossing it certainly warrant further exploration for gold, silver and copper. Northumberland Ø, where the Formation has its maximum thickness in Greenland, is an obvious target.

The red bed type copper mineralisation in sandstones of the Qaanaaq Formation of the Baffin Bay Group is probably of diagenetic origin, perhaps controlled by local faults. Only modest metal concentrations are indicated here, and it constitutes a low-priority exploration target.

The carbonates of the Dundas Group with their zinc mineralisation, albeit of modest size, show a potential for carbonate-hosted lead-zinc deposits, and in this respect it is worth noting that extensive outcrops of the group (Steensby Land Formation) occur south of the

Qaanaaq region. Also of relevance is the fact that commercial lead-zinc concentrations exist in carbonate rocks of comparable age at Nanisivik in the coeval Borden Basin of Baffin Island, Canada (Olson 1984).

No signs of gold-bearing shear zones were observed in the crystalline shield, but they might well exist. The syn- to post-depositional faults of the Thule Basin may be mineralised with quartz, baryte and pyrite, and associated with red bed mineralisation in sandstones and volcaniclastic rocks.

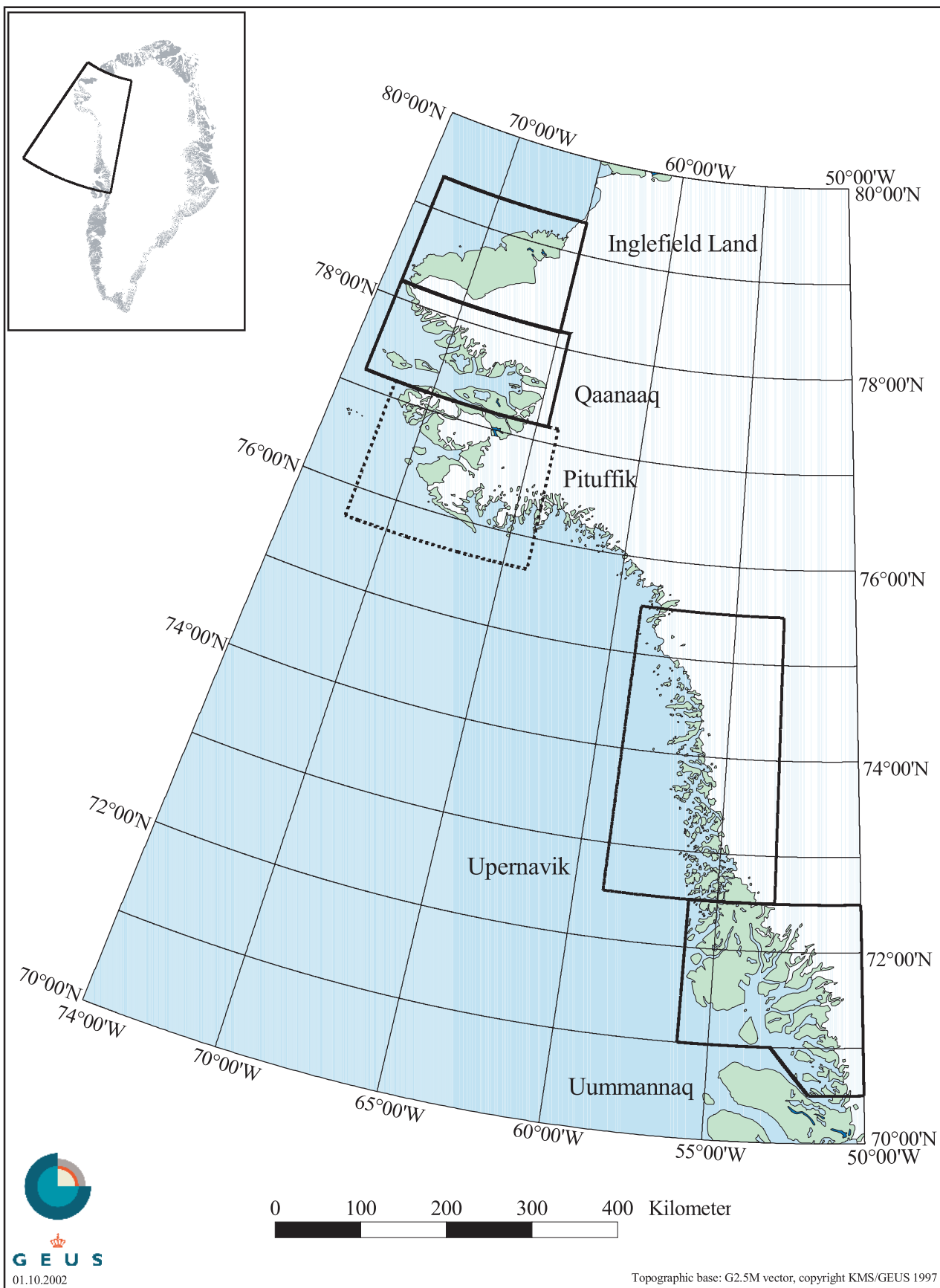
9. Acknowledgments

We acknowledge the help and support of the following persons during the field programme: Jes Burghardt, Nuuk, skipper of M/S *Kissavik* and his crew, pilot Glenn Lindström, Grønlandsfly A/S, field assistants Piuaitsoq Petersen and Peter Peary Aleqatsiaq from Qaanaaq, Hans and Birthe Jensen and company, Hotel Qaanaaq and Svend Erik Ascanus, Geophysical Observatory of the Danish Metrological Institute, Qaanaaq.

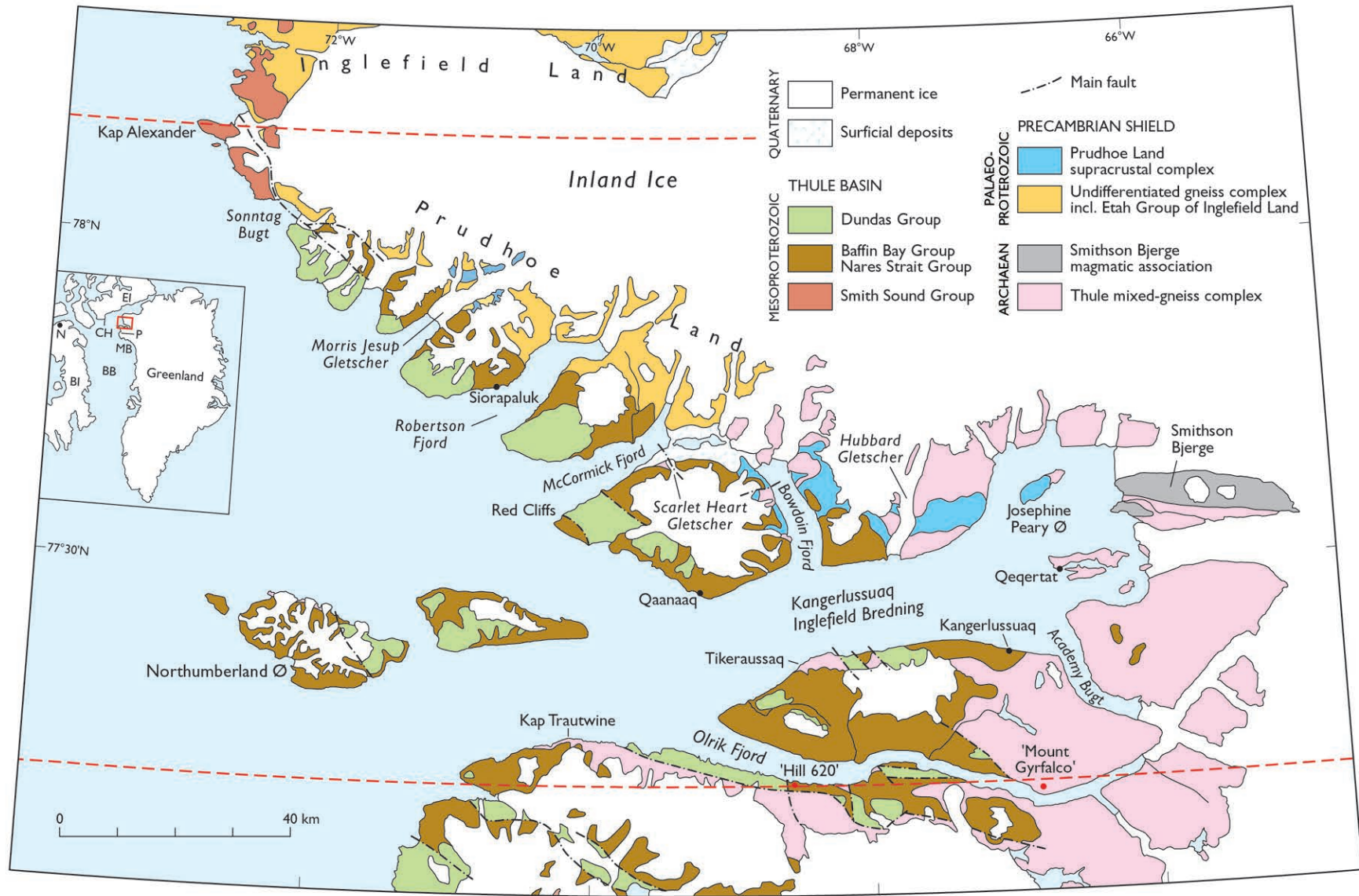
10. References

- Cooke, H.R. 1978: Mineral reconnaissance of the Thule district, North-West Greenland. Rapport Grønlands Geologiske Undersøgelse **90**, 17–22.
- Crippen, R.E. 1989: Selection of Landsat TM band and band-ratio combinations to maximize lithologic information in colour composite displays. Proceedings of the 7th thematic conference on remote sensing for exploration geology, Calgary, Canada, Oct. 2–6, 917–921. Michigan, USA: Environmental Research Institute of Michigan.
- Crosta, A.P. & McMoore, J. 1989: Enhancement of landsat thematic imagery for residual soil mapping in SW Minais Gerais State, Brazil: a prospecting case history in greenstone belt terrain. Proceedings of the 7th thematic conference on remote sensing for exploration geology, Calgary, Canada, Oct. 2–6, 1173–1187. Michigan, USA: Environmental Research Institute of Michigan.
- Dawes, P.R. 1976: 1:500 000 mapping of the Thule district, North-West Greenland. Rapport Grønlands Geologiske Undersøgelse **80**, 23–28.
- Dawes, P.R. 1988: Geological map of the Thule district, North-West Greenland, 1:100 000, sheets Siorapaluk, Qaanaaq, Hvalsund, Olrik Fjord and 1:200 000, sheet Inglefield Bredning. Unpublished maps, Geological Survey of Greenland (in archives of Geological Survey of Denmark and Greenland).
- Dawes, P.R. 1991: Geological map of Greenland, 1:500 000, Thule, sheet 5. Copenhagen: Geological Survey of Greenland.
- Dawes, P.R. 1997: The Proterozoic Thule Supergroup, Greenland and Canada: history, lithostratigraphy and development. *Geology of Greenland Survey Bulletin* **174**, 150 pp.
- Dawes, P.R. & Frisch, T. 1981: Geological reconnaissance of the Greenland shield in Melville Bugt, North-West Greenland. Rapport Grønlands Geologiske Undersøgelse **105**, 18–26.
- Dawes, P.R. *et al.* 2000: Kane Basin 1999: mapping, stratigraphic studies and economic assessment of Precambrian and Lower Palaeozoic provinces in north-western Greenland. *Geology of Greenland Survey Bulletin* **186**, 11–28.
- Dunnells, D. 1995: Ujarassiorit: 1989 to 1994. A summary report of years 1–6, 41 pp. Unpublished report, Nunaoil A/S, Nuuk, Greenland (in archives of Geological Survey of Denmark and Greenland, GEUS Report File 21421).
- Frisch, T. & Christie, R.L. 1982: Stratigraphy of the Proterozoic Thule Group, southeastern Ellesmere Island, Arctic Archipelago. *Geological Survey of Canada Paper* **81-19**, 12 pp.
- Gowen, J. & Kelly, J.G. 1996: Follow-up mineral exploration in the Thule area, North West Greenland, 1995, 10 pp. Unpublished report, Nunaoil A/S, Nuuk, Greenland (in archives of Geological Survey of Denmark and Greenland, GEUS Report File 21449).
- Gowen, J. & Sheppard, B. 1994: Reconnaissance mineral exploration in the Thule area, North West Greenland, 24 pp. Unpublished report, Nunaoil A/S, Nuuk, Greenland (in archives of Geological Survey of Denmark and Greenland, GEUS Report File 21418).
- Hunt, G.R. 1977: Spectral signatures of particulate minerals in the visible and near infrared. *Geophysics* **42**(3), 501–513.
- Jackson, G.D. 1986: Notes on the Proterozoic Thule Group, northern Baffin Bay. *Geological Survey of Canada Paper* **86-1A**, 541–552.
- Jackson, G.D. 2000: Geology of the Clyde–Cockburn Land map area, north-central Baffin Island, Nunavut. *Geological Survey of Canada Memoir* **440**, 303 pp. + 7 figs.

- Kirkham, R.V. 1996: Volcanic redbed copper. In: Eckstrand, O.R., Sinclair, W.D. & Thorpe, R.I. (eds): *Geology of Canadian mineral deposit types*. *Geology of Canada* **8**, 241–252. Ottawa: Geological Survey of Canada (also *The geology of North America P-1*, Geological Society of North America).
- Loughlin, W.P. 1991a: Principal component analysis for alteration mapping. *Photogrammetric Engineering & Remote Sensing* **57**(9), 1163–1169.
- Loughlin, W.P. 1991b: Principal component analysis for alteration mapping. *Proceedings of the 8th thematic conference on geologic remote sensing: exploration, engineering and environment* **1**, 293–306. Michigan, USA: Environmental Research Institute of Michigan.
- Nutman, A.P. 1984: Precambrian gneisses and intrusive anorthosite of Smithson Bjerge, Thule district, North-West Greenland. *Rapport Grønlands Geologiske Undersøgelse* **119**, 31 pp.
- Olsen, H.K. 2002: Ujarassiorit 2001. The mineral hunt in Greenland, 29 pp. Unpublished report, Greenland Resources A/S, Nuuk, Greenland.
- Olson, R.A. 1984: Genesis of paleokarst and strata-bound zinc-lead sulfide deposits in a Proterozoic dolostone, northern Baffin Island, Canada. *Economic Geology* **79**, 1056–1103.
- Steenfelt, A., Thomassen, B., Lind, M. & Kyed, J. 1998: Karrat 97: reconnaissance mineral exploration in central West Greenland. *Geology of Greenland Survey Bulletin* **180**, 73–80.
- Steenfelt, A., Dawes, P.R., Krebs, J.D., Moberg, E. & Thomassen, B. 2002: Geochemical mapping of the Qaanaaq region, 77°10' to 78°10' N, North-West Greenland. *Danmarks og Grønlands Geologiske Undersøgelse Rapport* **2002/65**, 29 pp. + 48 maps.
- Stuart Smith, J.H. & Campbell, D.L. 1971: The geology of Greenland north of latitude 74°30' N. Report No. 2, **2**. Mineral prospects of northern Greenland, 62 pp. + 3 map folios. Unpublished report, J.C. Sproule and Associates Ltd., Calgary, Canada for Greenarctic Consortium (in archives of Geological Survey of Denmark and Greenland, GEUS Report File 20811).
- Thomassen, B. 2001: Feltrapport for Qaanaaq 2001 projektet. September 2001. *Danmarks og Grønlands Geologiske Undersøgelse Rapport* **2001/101**, 8 pp.
- Thomassen, B. & Dawes, P.R. 1996: Inglefield Land 1995: geological and economic reconnaissance in North-West Greenland. *Bulletin Grønlands Geologiske Undersøgelse* **172**, 62–68.
- Thomassen, B. & Krebs, J.D. 2001: Guidelines for mineral exploration during the Qaanaaq 2001 project, 4 pp. Internal GEUS-notat, GEUS File no. 071-195.
- Thomassen, B., Dawes, P.R., Steenfelt, A. & Krebs, J.D. 2002: *Qaanaaq 2001*: mineral exploration reconnaissance in North-West Greenland. *Geology of Greenland Survey Bulletin* **191**, 133–143.

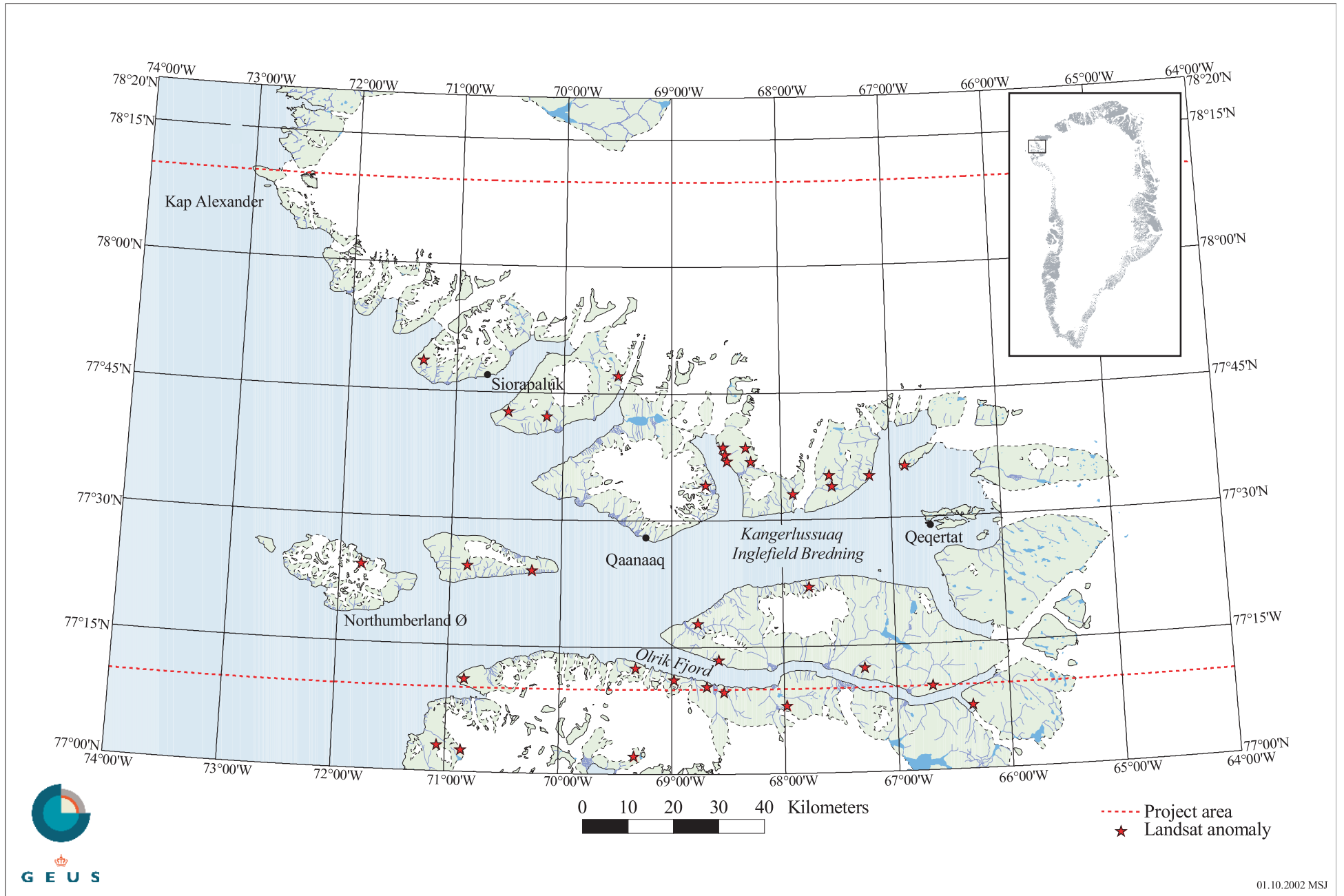


Map 1. Mineral reconnaissance projects accomplished (full frames) and planned (stippled frame).



Map 2. Geological map of the Qaanaaq region with project limits shown by red dashed lines. Basic sills, that in some areas of the Dundas Group form large outcrops, are not shown. Only faults affecting disposition of groups of the Thule Supergroup are depicted. Black dots are settlements; red dots other localities. Inset map: BB, Baffin Bay; BI, Baffin Island; CH, Clarence Head; EL, Ellesmere Island; MB, Melville Bugt; N, Nanisivik; P, Pituffik (Thule Air Base). Modified from Thomassen et al. (2002).

GN01.02-028-BTH/ld



Map 3. Landsat anomaly map.

Map 4. Sample locality and place name map

- Town/settlement
- Qaanaaq 2001 project area
- Rock sample locality

Danmarks og Grønlands Geologiske Undersøgelse Rapport 2002/88
 Topographic base: G/250 Vector, Copyright Kort & Matrikaltjenesten, 1998. UTM Zone 20.





Figure 1. *The basic logistics of Qaanaaq 2001 with typical weather: M/S Kissavik and rubber dinghies with overcast, low cloud and rain, Olrik Fjord in late August.*



Figure 2. *Helicopter-supported stream-sediment sampling at central Smithson Bjerge. In the background, south-facing rusty paragneiss and white anorthosite.*



Figure 3. *Basement–cover relationship. The Archaean Thule mixed-gneiss complex overlain by the Mesoproterozoic Thule Supergroup and cut by a Neoproterozoic dolerite dyke. The dark unit in the lower part of the cover is the volcanic Cape Combermere Formation. Kap Trautwine viewed from the north; height of cliff c. 800 m.*



Figure 4. *Basement–cover relationship in the crystalline shield. Rusty-weathering supracrustal rocks of the Palaeoproterozoic Prudhoe Land supracrustal complex overlying darker gneisses of the Archaean Thule mixed-gneiss complex. View from the south-east of the 770 m high Qattarsuit.*



Figure 5. Site of BIF scree blocks, e.g. 485815, from the Archaean Thule mixed-gneiss complex at Kap Trautwine.



Figure 6. Cut surface of BIF block with 24.4% Fe from Kap Trautwine (485815). Match is 5 cm. Photo: Jakob Lautrup.



Figure 7. Aerial view eastwards of the BIF showing in tightly folded, rusty gneisses of the Thule mixed-gneiss complex north-east of 'Mount Gyrfalco'. The cliff with the rusty scree in the left foreground is about 400 m high.



Figure 8. Aerial view westwards of the BIF showing north-east of 'Mount Gyrfalco', with isoclinal fold hinge in the foreground.



Figure 9. Typical BIF with 26.4% Fe from the 'Mount Gyrfalco' showing (485733). Match is 5 cm. Photo: Jakob Lautrup.



Figure 10. Cut surface of BIF with 29.3% Fe from the 'Mount Gyrfalco' showing (485732). Match is 5 cm. Photo: Jakob Lautrup.



Figure 11. Aerial view towards the west in central Smithson Bjerge. Rusty paragneiss with BIF is intruded by white anorthosite. Relief is about 500 m.



Figure 12. A coastal cliff about 600 m high of mixed orthogneisses and paragneisses with malachite staining (not visible on the picture) south-west of Qattarsuit. Samples 485748–57 were collected in exposure and scree in the middle of the picture.



Figure 13. Typical colour anomaly in the Prudhoe Land supracrustal complex. View eastwards with Gable Gletscher in the background. Samples 485761–65 were collected at centre of picture.



Figure 14. Typical graphite-pyrite schist, west of Gable Gletscher (485761). Logo is 8.5 cm.



Figure 15. *Cut surface of neosome quartz from graphite-pyrite schist showing mesh of pyrite (485763). Match is 5 cm. Photo: Jakob Lautrup.*



Figure 16. *Cut surface of graphite-pyrite schist (485772). Note abundant shining grey graphite, yellow pyrite with quartz concentrated in fold hinge. Match is 5 cm. Photo: Jakob Lautrup.*



Figure 17. Quartzite from the Prudhoe Land supracrustal complex showing folded pelite band and malachite staining. Nunatak north of Morris Jesup Gletscher, sample 485716.



Figure 18. Cut surface of volcanic agglomerate with 1% Cu from Cape Combermere Formation, Northumberland Ø (485795). Match is 5 cm. Photo: Jakob Laurup.



Figure 19. Aerial view towards the west along the south coast of Olrik Fjord with the 'Hill 620' showing in the foreground as a yellow patch. For geology description, see Frontispiece.

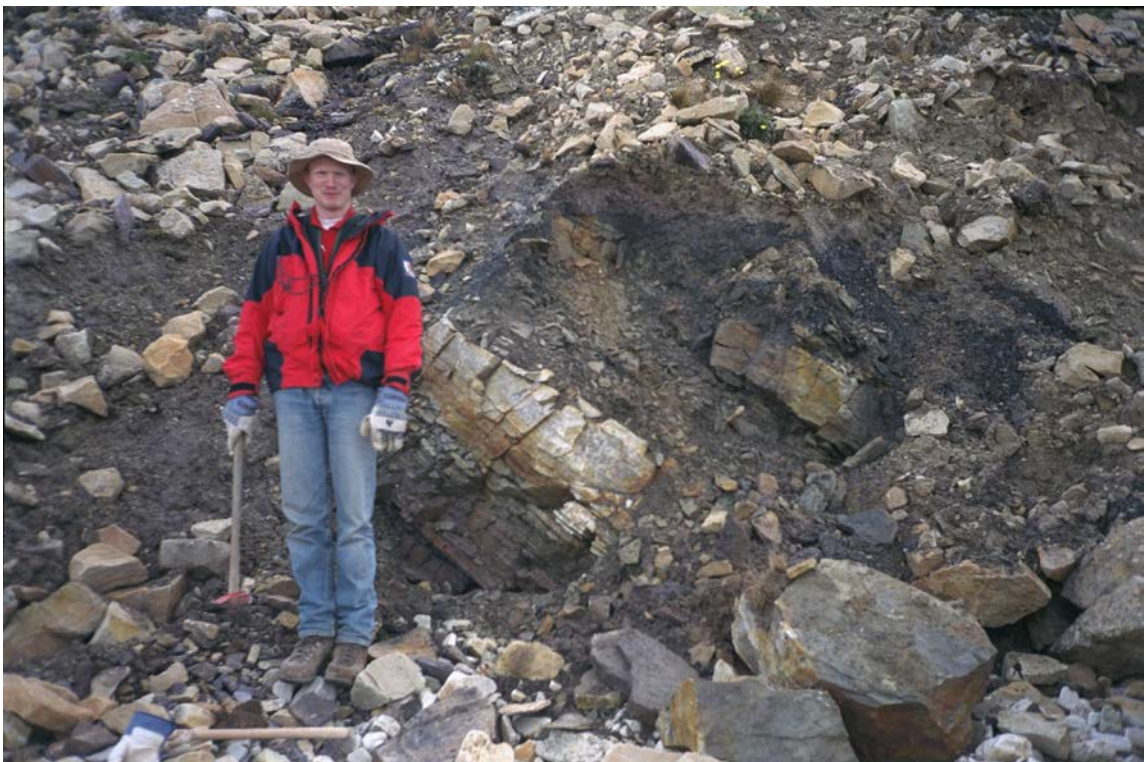


Figure 20. Red Cliffs: shale–sandstone unit of the Qaanaaq Formation to the right of JDK displays faint malachite staining (not seen on picture) and yielded 1.5% Cu in a composite sample (485712).



Figure 21. *Interbedded dark shales and stromatolitic carbonate beds, Dundas Group, Northumberland Ø. The base of the carbonate bed (at the notebook) contains minor sphalerite and a composite sample returned 2% Zn (485786).*



Figure 22. *Quartz veins with minor chalcopyrite in gneisses of the Archaean Thule mixed-gneiss complex at Tikeraasaq (485718).*

Table 1. *Rock sample list*

GGU no.	W Long.	N Lat.	Alt. m	Type	Geol. unit	Field description
470001	-71.9699	77.9173	60	b	U	Paragneiss with py.
470002	-71.9535	77.9179	80	b	D	Sandstone with py.
470003	-72.2296	78.0418	10	b	U	Paragneiss with py. and cpy.
470004	-72.2293	78.0487	60	b	U	Siliceous rock with py. and graphite
470005	-72.2319	78.0474	10	b	U	Paragneiss with py. and cpy.
470006	-72.2363	78.0449	10	b	U	Paragneiss with py.
470007	-72.2005	78.0367	10	b	U	Paragneiss with py. and graphite
470008	-72.1704	78.0315	130	b	U	Paragneiss with py.
470009	-71.1150	77.8763	80	b	V	Dolerite with mag. and iron sulphides
470010	-69.4442	77.7505	15	b	U	Dolerite with iron- and copper sulphides
470020	-65.5378	77.5618	350	b	T	Quartz-rich rock with py.
470021	-67.7832	77.5223	30	b	T	Quartzite with py.
470022	-67.7809	77.5237	30	b	T	Quartzite with mag.
470023	-67.7809	77.5237	30	b	T	Quartzite with py.
470024	-68.3394	77.6030	250	b	P	Quartzite with py.
470025	-68.3395	77.6037	270	b	P	Quartz-feldspar rock with py.
470026	-70.3347	77.8647	50	b	U	Quartzite with py.
470027	-71.5460	77.3841	130	o	D	Shale with py.
470028	-71.5025	77.3794	230	bc	D	Brecciated rock with cpy.
470029	-69.9566	77.2295	30	b	T	Ultramafic rock with py.
470030	-70.1196	77.5517	10	b	B	Sandstone with py.
485701	-72.0626	77.9329	20	b	U	Gneiss with pyrrh. and trace cpy.
485702	-71.9931	77.9346	60	b	U	Garnet quartzite with minor pyrrh.
485703	-72.1921	78.0175	90	b	U	Gneiss with pyrrh. and trace cpy.
485704	-72.1921	78.0175	90	b	U	Siliceous gneiss with pyrrh.
485705	-72.1518	78.0140	120	b	U	Garnet gneiss with pyrrh., trace cpy.
485706	-72.1518	78.0140	120	b	U	Gneiss with pyrrh., trace cpy.
485707	-71.2699	77.8871	10	b	P	Marble with trace cpy.
485708	-71.2642	77.8890	2	b	V	Massive graphite with garnet and vqz.
485709	-69.4693	77.7748	100	b	T	BIF.
485710	-69.4800	77.7667	110	b	U	Metagabbro with pyrrh., cpy., and mag.
485711	-70.2574	77.5757	25	oc	B	White sandstone with mal.
485712	-70.2437	77.5770	3	oc	B	Shale with mal. and cpy.
485713	-70.2341	77.5782	10	b	B	Sandstone with py.
485714	-69.5687	77.7348	125	b	B	White sandstone with mal.
485715	-70.6958	77.9628	380	o	P	Ultramafic rock: mal. and trace sulphides.
485716	-70.7022	77.9663	680	o	P	Quartzite with mal. and trace cpy.
485717	-68.4636	77.3467	145	b	V	Siliceous breccia with trace cpy.
485718	-68.4607	77.3466	140	oc	V	Vqz. with trace cpy.
485719	-68.4723	77.3478	130	b	T	Paragneiss with trace py.
485720	-68.3332	77.6832	530	c 1.0	P	Graphite schist with py.

GGU no.	W Long.	N Lat.	Alt. m	Type	Geol. unit	Field description
485721	-68.3334	77.6832	530	o	P	Quartzite with py.
485722	-65.6192	77.5656	350	b	T	BIF.
485723	-65.6192	77.5656	350	b	T	BIF.
485724	-65.6192	77.5656	350	b	T	BIF.
485725	-65.6192	77.5656	350	b	T	BIF.
485726	-68.5568	77.1713	150	bc	B	Qaanaaq Fm. sandstone with mal.
485727	-68.9169	77.1774	210	oc	V	Vqz. with trace py.
485728	-68.9169	77.1774	210	oc	V	Vqz. with trace py.
485729	-66.6885	77.1704	570	c 1.5	T	Massive mag. with pyrrh.
485730	-66.6885	77.1704	570	c 2.0	T	Mag.-rich rock: BIF.
485731	-66.6885	77.1704	570	c 3.0	T	BIF.
485732	-66.6885	77.1704	570	o	T	BIF.
485733	-66.6885	77.1704	570	o	T	BIF.
485734	-66.6885	77.1704	570	o	T	BIF.
485735	-66.1772	77.2919	190	o	T	Hornblendite with mal. and mag.
485736	-66.8070	77.3608	50	b	T	Breccia with trace py.
485737	-66.8070	77.3608	50	b	T	Breccia with trace py.
485738	-66.8070	77.3608	50	b	T	Altered mafic rock with py.
485739	-66.2505	77.2880	2	o	T	Ultramafic rock with vqz. and trace py.
485740	-66.2271	77.4297	25	b	T	High-strain gneiss with mag.
485741	-66.1568	77.5886	30	b	T	Quartzite with pyrrh.
485742	-66.1568	77.5886	30	b	T	Garnet-vqz rock with pyrrh.
485743	-66.1568	77.5886	40	b	T	Garnet quartzite with pyrrh. and trace cpy.
485744	-66.1494	77.5966	50	b	T	Garnet quartzite with pyrrh.
485745	-66.1434	77.5999	25	b	T	Garnet-hornbl. quartzite with pyrrh.
485746	-66.1616	77.5966	2	b	T	Garnet quartzite with pyrrh.
485747	-66.1616	77.5966	3	b	T	Garnet-hornbl. quartzite with pyrrh.
485748	-67.4152	77.5415	10	b	T	Melanocratic paragneiss: mal., trace cpy.
485749	-67.4152	77.5415	15	b	T	Melanocratic paragneiss: mal., trace sulph.
485750	-67.4152	77.5415	20	o	T	Quartzite with mal. and sulphides.
485751	-67.4152	77.5415	5	b	T	Garnet-quartz paragneiss with pyrrh.
485752	-67.4152	77.5415	5	b	T	Garnet-quartz paragneiss with pyrrh.
485753	-67.4152	77.5415	5	b	T	Garnet-quartz paragneiss with pyrrh.
485754	-67.4152	77.5415	10	b	T	Garnet-quartz paragneiss with pyrrh.
485755	-68.5417	77.6732	30	b	T	Garnet quartzite with pyrrh. and trace cpy.
485756	-68.5417	77.6732	30	b	T	Garnet quartzite with sulphides.
485757	-68.5417	77.6732	30	b	T	Strained gneiss: mag., dissem. sulph.
485758	-68.5417	77.6732	30	b	T	Garnet quartzite with sulphides.
485759	-68.5417	77.6732	30	b	T	Garnet quartzite with graphite and pyrrh.
485760	-68.8279	77.6777	50	b	T	Garnet quartzite with pyrrh.
485761	-68.2940	77.6035	170	o	P	Graphite schist.
485762	-68.2940	77.6035	170	o	P	Graphite schist with py.
485763	-68.2940	77.6035	170	b	P	Neosome with py.
485764	-68.2940	77.6035	170	b	P	Neosome with py.

GGU no.	W Long.	N Lat.	Alt. m	Type	Geol. unit	Field description
485765	-68.2940	77.6035	170	b	P	Neosome with py.
485766	-67.8952	77.5298	100	b	T	BIF with trace sulphides.
485767	-67.8975	77.5311	100	b	T	Amphibolite with sulphides.
485768	-67.8977	77.5341	100	b	T	Paragneiss with sulphides.
485769	-67.8977	77.5341	100	b	T	BIF with trace sulphides.
485770	-67.8977	77.5341	100	b	T	BIF with trace sulphides.
485771	-67.8977	77.5341	100	b	T	BIF with trace sulphides.
485772	-68.4850	77.6171	60	b	P	Graphite schist with py.
485773	-68.4850	77.6171	100	b	P	Amphibolite with py.
485774	-70.5608	77.8327	50	b	U	Sheared rock with py.
485775	-70.5369	77.8287	40	b	U	Quartz-banded rock with py.
485776	-70.2885	77.8687	100	b	U	Amphibolite with disseminated py.
485777	-70.2850	77.8648	70	b	U	Gneiss with trace cpy.
485778	-70.2850	77.8648	70	b	U	Amphibolite with disseminated py.
485779	-70.2850	77.8648	70	b	U	Amphibolite with disseminated py.
485780	-70.0982	77.8527	10	b	U	Ultramafic rock with dissem. sulphides.
485781	-70.0982	77.8527	10	b	U	Garnet-quartz rock with pyrrh.
485782	-69.9941	77.8540	10	b	U	Garnet quartzite with sulphides.
485783	-71.6197	77.3923	130	b	B	Sandstone with minor py. and trace cpy.
485784	-71.6197	77.3923	130	b	B	Sandstone with py. and mal.
485785	-71.5522	77.3856	100	b	D	Sandstone with py.
485786	-71.4896	77.3775	110	oc	D	Limestone with minor sp.
485787	-71.4896	77.3775	110	oc	D	Black shale with py.
485788	-71.4840	77.3811	90	b	D	Shaly sandstone with py.
485789	-71.5074	77.3844	50	b	D	Sandstone with py.
485790	-71.5193	77.3852	50	b	D	Carbonate breccia with py
485791	-71.8244	77.4203	60	b	N	Volcanic breccia with hem. and mal.
485792	-71.8244	77.4203	60	b	N	Volcanic breccia with hem.
485793	-71.8244	77.4203	60	b	N	Volcanic breccia with hem.
485794	-71.8244	77.4203	60	b	N	Vesicular lava with mal.
485795	-71.8244	77.4203	60	b	N	Volcanic breccia with mal.
485796	-71.8244	77.4203	60	b	N	Dolerite with mal.
485797	-66.8900	77.1518	5	b	T	Garnet-quartz rock with minor sulphides.
485798	-66.4904	77.1650	30	b	T	Ultramafic rock with py.
485799	-66.4904	77.1650	30	b	T	Amphibolite with py.
485800	-66.2864	77.1798	10	b	T	Ultramafic rock with py.
485801	-66.3406	77.1586	60	b	T	Garnet amphibolite with pyrrh.
485802	-66.3406	77.1586	60	b	T	Gneiss with pyrrh.
485803	-66.3406	77.1586	60	b	T	Gneiss with pyrrh.
485804	-69.1942	77.2014	100	b	D	Sandstone with py.
485805	-69.2088	77.1994	120	b	T	Amphibolite with pyrrh. and trace cpy.
485806	-69.2263	77.1936	190	b	T	Quartz-banded rock: pyrrh. and trace cpy.
485807	-69.2263	77.1936	190	b	T	Gneiss with pyrrh. and trace cpy.
485808	-69.2263	77.1936	190	b	T	Mafic rock with pyrrh. and trace cpy.

GGU no.	W Long.	N Lat.	Alt. m	Type	Geol. unit	Field Description
485809	-69.2263	77.1936	190	b	T	Ultramafic rock: pyrrh., py. and trace cpy.
485810	-69.2263	77.1936	190	b	T	Mafic rock with pyrrh., pyrrh. and trace cpy.
485811	-70.2812	77.2287	30	b	T	Gneiss with pyrrh.
485812	-70.1756	77.2404	25	b	T	Gneiss with iron-sulphides.
485813	-70.1756	77.2404	25	b	T	Gneiss with iron-sulphides.
485814	-70.1756	77.2404	25	b	T	Amphibolite with py.
485815	-70.1756	77.2404	25	b	T	BIF.
485816	-70.1200	77.2409	5	b	T	Sulphide-lens in gneiss.
485817	-70.1200	77.2409	5	b	T	Gneiss with disseminated pyrrh.
485818	-70.1200	77.2409	5	b	T	Mag.-lens in gneiss.
485819	-70.1200	77.2409	5	b	T	BIF.
485820	-70.1200	77.2409	5	b	T	BIF.
485821	-70.1200	77.2409	5	b	T	BIF.
485822	-70.0429	77.2374	10	b	T	Py.-quartz vein in gneiss
485823	-69.5204	77.2104	90	b	T	Hornblendite with iron-sulphides.
485824	-69.5215	77.2086	90	b	T	Hornblendite with pyrrh. and trace cpy.
485825	-69.5215	77.2086	90	b	T	Hornblendite with pyrrh. and trace cpy.
485826	-69.5215	77.2086	90	b	T	Gneiss with pyrrh. and trace cpy.
485827	-69.5215	77.2086	90	b	T	Gneiss with pyrrh. and trace cpy.
485828	-69.5278	77.2062	100	b	T	Vqz. with minor pyrrh. and cpy. in gneiss.
485829	-69.5415	77.2047	180	b	T	Lens of pyrrh. and trace cpy. in gneiss.
485830	-69.1740	77.4588	3	oc	B	Sandstone with mal.
485831	-69.1740	77.4588	3	oc	B	Silty shale above previous sample.

Abbreviations

o	= sample from outcrop
oc	= composite sample from outcrop
b	= boulder or scree sample
bc	= composite boulder or scree sample
c1.0	= chip sample over 1.0 m
cpy.	= chalcopyrite
hem.	= hematite
mag.	= magnetite
mal.	= malachite
py.	= pyrite
pyrrh.	= pyrrhotite
sp.	= sphalerite
vqz.	= vein quartz
V	= Quartz vein or basic dyke
D	= Dundas Group
B	= Baffin Bay Group
N	= Nares Strait Group
P	= Prudhoe Land supracrustal complex
U	= Undifferentiated gneiss complex
T	= Thule mixed-gneiss complex

Table 2. *Rock samples: analytical results*

Element	Detection limit	Analytical method	Element	Detection limit	Analytical method
Ag	0.3 ppm	ICP	Mn	1 ppm	ICP
Au	2 ppb	INAA	Mo	1 ppm	ICP
Au	2 ppb	FA	Na	0.01 pct	INAA
Al	0.01 pct	INAA	Nd	5 ppm	INAA
As	0.5 ppm	INAA	Ni	1 ppm	ICP
Ba	50 ppm	INAA	P	0.001 pct	ICP
Be	1 ppm	ICP	Pb	3 ppm	ICP
Bi	2 ppm	ICP	Pd	4 ppb	FA
Br	0.5 ppm	INAA	Pt	5 ppb	FA
Ca	0.01 pct	ICP	Rb	15 ppm	INAA
Cd	0.3 ppm	ICP	S	0.001 pct	ICP
Ce	3 ppm	INAA	Sb	0.1 ppm	INAA
Co	1 ppm	INAA	Sc	0.1 ppm	INAA
Cr	5 ppm	INAA	Se	3 ppm	INAA
Cs	1 ppm	INAA	Sm	0.1 ppm	INAA
Cu	1 ppm	ICP	Sn	0.01 pct	INAA
Eu	0.2 ppm	INAA	Sr	0.5 ppm	ICP
Fe	0.01 pct	INAA	Ta	0.5 ppm	INAA
Hf	1 ppm	INAA	Tb	0.5 ppm	INAA
Hg	1 ppm	INAA	Th	0.2 ppm	INAA
Ir	5 ppb	INAA	Ti	0.01 pct	ICP
K	0.01 pct	ICP	U	0.5 ppm	INAA
La	0.5 ppm	INAA	V	2 ppm	ICP
Lu	0.05 ppm	INAA	W	1 ppm	INAA
Mg	0.01 pct	ICP	Y	1 ppm	ICP
			Yb	0.2 ppm	INAA
			Zn	1 ppm	ICP

Analysis by Activation Laboratories Ltd., Ontario, Canada.

Analytical methods:

INAA: Instrumental neutron activation

ICP: Inductively coupled plasma emission spectrometry

FA: Fire assay

GGU no.	Au ppb	Au ppb(FA)	Ag ppm	Pt ppb	Pd ppb	Ir ppb	As ppm	Sb ppm	Se ppm	Hg ppm
470001	13		0.4			<5	<0.5	0.3	<3	<1
470002	2		<0.3			<5	0.9	0.1	<3	<1
470003	<2		6.7			<5	7.6	0.2	4	<1
470004	101	51	0.5	<5	19	<5	1.8	<0.1	<3	<1
470005	26	29	2.5	<5	6	<5	<0.5	<0.1	4	<1
470006	<2		1.0			<5	<0.5	<0.1	10	<1
470007	<2		1.1			<5	<0.5	<0.1	<3	<1
470008	5		1.9			<5	4.0	<0.1	12	<1
470009	5		1.2			<5	<0.5	<0.1	<3	<1
470010	<2	5	0.6	<5	6	<5	1.5	<0.1	<3	<1
470020	17		1.1			<5	39.9	<0.1	<3	<1
470021	8		<0.3			<5	1.2	<0.1	<3	<1
470022	<2		<0.3			<5	<0.5	<0.1	<3	<1
470023	<2	6	<0.3	6	20	<5	<0.5	0.3	<3	<1
470024	<2		0.4			<5	4.9	<0.1	9	<1
470025	4		0.5			<5	1.6	<0.1	<3	<1
470026	37	32	0.9	<5	6	<5	<0.5	<0.1	<3	<1
470027	3		0.3			<5	5.8	0.4	<3	<1
470028	<2		<0.3			<5	2.5	0.1	<3	<1
470029	3		<0.3			<5	1.0	0.2	<3	2
470030	7		0.8			<5	98.1	0.5	<3	<1
485701	60	76	1.7	<5	12	<5	1.4	<0.1	4	<1
485702	3		0.3			<5	<0.5	<0.1	<3	<1
485703	<2		1.0			<5	<0.5	<0.1	<3	<1
485704	<2		0.5			<5	<0.5	<0.1	<3	<1
485705	<2		0.8			<5	2.1	<0.1	<3	<1
485706	6		1.1			<5	1.5	<0.1	<3	<1
485707	6		<0.3			<5	1.6	<0.1	<3	<1
485708	<2		<0.3			<5	<0.5	<0.1	<3	<1
485709	<2		<0.3			<5	<0.5	<0.1	<3	<1
485710	10	7	<0.3	<5	<4	<5	<0.5	<0.1	<3	<1
485711	6		<0.3			<5	4.9	0.1	<3	<1
485712	2		0.7			<5	2.5	0.1	<3	<1
485713	<2		<0.3			<5	21.1	0.3	<3	<1
485714	<2		<0.3			<5	2.0	<0.1	<3	<1
485715	<2	3	0.8	<5	<4	<5	2.1	<0.1	<3	2
485716	<2		0.5			<5	3.2	<0.1	<3	<1
485717	2		<0.3			<5	2.7	0.3	<3	<1
485718	<2		<0.3			<5	<0.5	0.3	<3	<1
485719	<2		1.1			<5	4.8	0.3	<3	<1
485720	<2		<0.3			<5	<0.5	<0.1	<3	<1
485721	<2		<0.3			<5	1.8	<0.1	<3	<1

GGU no.	Au ppb	Au ppb(FA)	Ag ppm	Pt ppb	Pd ppb	Ir ppb	As ppm	Sb ppm	Se ppm	Hg ppm
485722	4		<0.3			<5	2.1	<0.1	<3	<1
485723	19	13	<0.3	<5	<4	<5	39.4	<0.1	<3	<1
485724	4		<0.3			<5	2.7	<0.1	<3	<1
485725	<2		<0.3			<5	1.3	0.2	<3	<1
485726	<2		5.3			<5	30.6	0.3	<3	<1
485727	3		<0.3			<5	4.3	<0.1	<3	<1
485728	3		<0.3			<5	2.5	<0.1	<3	<1
485729	7	19	0.4	<5	5	<5	6.4	<0.1	<3	<1
485730	5	4	<0.3	6	<4	<5	6.8	<0.1	<3	<1
485731	2	6	<0.3	<5	<4	<5	11.4	<0.1	<3	<1
485732	<2		<0.3			<5	3.5	<0.1	<3	<1
485733	<2		<0.3			<5	4.3	<0.1	<3	<1
485734	<2		<0.3			<5	3.9	<0.1	<3	<1
485735	4	3	<0.3	<5	<4	<5	<0.5	<0.2	<3	<1
485736	<2		<0.3			<5	2.5	<0.1	<3	<1
485737	<2		<0.3			<5	4.9	<0.1	<3	<1
485738	<2		0.4			<5	1.3	<0.1	<3	<1
485739	<2		<0.3			<5	1.5	0.3	<3	3
485740	<2		0.3			<5	1.5	<0.1	<3	1
485741	19	23	0.4	<5	6	<5	1.7	<0.1	<3	<1
485742	<2		<0.3			<5	<0.5	<0.1	<3	<1
485743	102	83	0.4	<5	<4	<5	28.1	<0.1	<3	<1
485744	<2		<0.3			<5	1.5	<0.1	<3	<1
485745	14	9	<0.3	<5	<4	<5	8.8	<0.1	<3	<1
485746	<2		<0.3			<5	1.6	<0.1	<3	<1
485747	<2		<0.3			<5	1.8	<0.1	<3	<1
485748	<2	5	0.3	<5	4	<5	2.4	<0.1	<3	<1
485749	9		<0.3			<5	1.0	<0.1	<3	<1
485750	10		0.3			<5	2.7	<0.1	<3	<1
485751	<2		<0.3			<5	1.6	<0.1	<3	<1
485752	22		<0.3			<5	5.8	<0.1	<3	<1
485753	18	13	<0.3	<5	4	<5	56.3	<0.1	<3	<1
485754	14	11	<0.3	<5	<4	<5	2.0	<0.1	<3	<1
485755	<2		0.3			<5	3.1	0.2	<3	<1
485756	14	19	0.5	<5	<4	<5	2.5	<0.1	<3	<1
485757	<2		<0.3			<5	1.7	<0.1	<3	<1
485758	<2		<0.3			<5	2.4	<0.1	<3	<1
485759	<2		0.2			<5	2.1	<0.1	<3	<1
485760	<2		1.6			<5	1.5	<0.1	<3	<1
485761	<2		0.6			<5	1.7	<0.1	<3	<1
485762	5	4	2.5	<5	14	<5	3.2	<0.1	20	<1
485763	<2		<0.3			<5	1.2	0.1	9	<1
485764	<2		<0.3			<5	2.2	<0.1	15	<1
485765	4	6	<0.3	<5	<4	<5	3.1	<0.1	18	<1

GGU no.	Au ppb	Au ppb(FA)	Ag ppm	Pt ppb	Pd ppb	Ir ppb	As ppm	Sb ppm	Se ppm	Hg ppm
485766	<2		<0.3			<5	1.0	<0.1	<3	<1
485767	<2	<2	0.5	<5	<4	<5	<0.5	<0.1	<3	<1
485768	<2		<0.3			<5	2.1	<0.1	<3	<1
485769	11		<0.3			<5	1.6	<0.1	<3	<1
485770	3		<0.3			<5	1.8	<0.1	3	<1
485771	<2		<0.3			<5	1.7	<0.1	<3	<1
485772	12	11	0.5	<5	13	<5	2.6	<0.1	8	<1
485773	<2		0.6			<5	3.4	<0.1	8	<1
485774	<2		0.5			<5	1.6	<0.1	<3	<1
485775	<2		<0.3			<5	1.3	<0.1	<3	<1
485776	<2		<0.3			<5	<0.5	<0.1	<3	<1
485777	16	18	1.2	<5	<4	<5	5.3	<0.1	<3	<1
485778	<2		<0.3			<5	<0.5	<0.1	<3	<1
485779	<2		<0.3			<5	2.3	<0.1	<3	<1
485780	<2		<0.3			<5	4.2	<0.1	8	<1
485781	<2		0.5			<5	3.2	<0.1	5	1
485782	81	62	<0.3	6	8	<5	2.0	<0.1	<3	<1
485783	3		<0.3			<5	4.5	0.5	<3	<1
485784	<2		<0.3			<5	5.7	0.1	<3	<1
485785	<2		<0.3			<5	2.1	0.4	<3	<1
485786	<2		<0.3			<5	2.8	<0.1	<3	<1
485787	<2		0.3			<5	3.6	0.9	<3	<1
485788	<2		<0.3			<5	14.3	0.4	<3	<1
485789	<2		<0.3			<5	6.2	0.3	<3	<1
485790	5		<0.3			<5	6.9	0.3	<3	<1
485791	106	96	156.4	44	127	<5	12.2	0.5	20	<1
485792	<2		<0.3			<5	5.6	<0.1	<3	<1
485793	<2		<0.3			<5	5.8	0.5	<3	<1
485794	<2	<2	0.8	<5	4	<5	5.1	<0.1	<3	<1
485795	<2	2	10.6	<5	5	<5	2.4	<0.1	<3	<1
485796	<2		0.4			<5	2.3	<0.1	<3	<1
485797	4		<0.3			<5	1.5	<0.1	<3	<1
485798	<2	<2	<0.3	<5	10	<5	3.5	<0.1	<3	<1
485799	<2		<0.3			<5	<0.5	<0.1	<3	<1
485800	<2		<0.3			<5	<0.5	<0.1	<3	<1
485801	32	31	0.5	8	19	<5	1.9	<0.1	<3	<1
485802	5		0.4			<5	1.6	<0.1	<3	<1
485803	5	2	0.9	<5	<4	<5	1.4	<0.1	<3	<1
485804	2		0.5			<5	3.2	0.2	<3	<1
485805	<2		0.5			<5	1.0	<0.1	5	<1
485806	14	9	0.9	6	9	<5	2.2	<0.1	<3	<1
485807	8		0.5			<5	1.5	<0.1	<3	<1
485808	<2		<0.3			<5	1.3	0.2	<3	<1
485809	<2	5	0.8	<5	<4	<5	1.8	<0.1	<3	<1

GGU no.	Au ppb	Au ppb(FA)	Ag ppm	Pt ppb	Pd ppb	Ir ppb	As ppm	Sb ppm	Se ppm	Hg ppm
485810	<2	5	0.6	<5	4	<5	2.7	<0.1	8	<1
485811	<2		1.0			<5	2.4	<0.1	6	<1
485812	<2		0.6			<5	<0.5	<0.1	<3	<1
485813	<2		0.8			<5	1.6	<0.1	<3	<1
485814	<2		<0.3			<5	2.1	<0.1	<3	<1
485815	<2		<0.3			<5	<0.5	<0.1	<3	<1
485816	<2	4	1.8	5	<4	<5	0.8	<0.1	<3	<1
485817	<2		0.5			<5	2.5	<0.1	<3	<1
485818	<2		<0.3			<5	<0.5	<0.1	<3	<1
485819	1		<0.3			<5	<0.5	<0.1	<3	<1
485820	<2	2	<0.3	<5	<4	<5	<0.5	<0.1	<3	<1
485821	<2		<0.3			<5	1.3	<0.1	<3	<1
485822	<2		<0.3			<5	1.8	<0.1	<3	<1
485823	3		0.4			<5	1.2	<0.1	<3	2
485824	<2	6	0.6	6	<4	<5	1.1	<0.1	<3	<1
485825	3		1.0			<5	2.6	<0.1	<3	<1
485826	36	37	0.8	<5	9	<5	3.6	<0.1	<3	<1
485827	5		1.5			<5	1.8	<0.1	<3	<1
485828	<2		<0.3			<5	2.1	0.1	<3	<1
485829	<2	3	0.7	<5	<4	<5	1.9	<0.1	<3	2
485830	<2		0.8			<5	2.2	0.4	<3	<1
485831	4		1.8			<5	3.3	0.6	<3	<1
Samples	152	40	152	40	40	152	152	152	152	152
Minimum	<2	<2	<0.3	<5	<4	<5	<0.5	<0.2	<3	<1
Maximum	106	96	156.4	44	127	<5	98.1	0.9	20	3
Median	<2	7	<0.3	<5	4	<5	2.0	<0.1	<3	<1

GGU no.	Cu ppm	Pb ppm	Zn ppm	Cd ppm	Bi ppm	Mo ppm	Ni ppm	Co ppm	Cr ppm	S pct
470001	270	28	50	<0.3	<2	12	77	48	80	1.107
470002	19	4	8	<0.3	<2	<1	3	2	<5	1.815
470003	354	<3	234	<0.3	<2	33	239	110	469	3.874
470004	1664	5	213	<0.3	<2	15	576	124	381	3.107
470005	1054	29	98	<0.3	<2	21	204	68	169	1.735
470006	362	10	75	<0.3	<2	109	145	81	120	3.779
470007	606	23	121	<0.3	<2	17	205	98	244	3.150
470008	676	37	56	<0.3	2	10	198	120	174	6.048
470009	312	<3	104	<0.3	<2	<1	63	44	70	0.199
470010	1901	<3	133	<0.3	<2	3	3582	211	2380	3.079
470020	359	7	132	<0.3	<2	6	186	55	97	4.429
470021	204	<3	80	<0.3	2	6	94	25	35	1.936
470022	109	<3	42	<0.3	5	6	51	8	36	0.579
470023	931	<3	238	<0.3	<2	9	3282	148	808	3.307
470024	43	15	304	<0.3	<2	2	82	13	62	0.215
470025	15	39	33	<0.3	3	3	42	34	15	5.929
470026	613	6	194	<0.3	3	22	335	119	405	2.941
470027	43	48	214	<0.3	3	2	48	19	22	3.129
470028	426	6	17	<0.3	<2	<1	17	5	27	0.065
470029	383	8	107	<0.3	<2	2	94	60	141	0.880
470030	17	11	6	<0.3	3	10	30	32	9	1.693
485701	1445	21	1769	<0.3	<2	42	1501	211	3250	4.575
485702	157	23	56	<0.3	<2	4	54	25	76	0.626
485703	283	41	61	<0.3	2	4	76	57	96	3.211
485704	376	26	37	<0.3	<2	4	41	37	11	1.433
485705	85	16	104	<0.3	<2	3	59	33	234	0.349
485706	694	9	86	<0.3	<2	2	74	47	114	1.993
485707	726	4	<1	<0.3	<2	<1	1	<1	<5	0.146
485708	20	7	45	<0.3	<2	1213	16	13	111	0.219
485709	24	<3	33	<0.3	5	8	27	7	31	0.091
485710	361	6	49	<0.3	<2	14	325	89	72	3.408
485711	7	<3	5	<0.3	<2	2	2	5	59	0.182
485712	15247	12	4	<0.3	<2	2	10	8	9	2.107
485713	15	5	7	<0.3	<2	6	1	1	5	0.824
485714	358	3	7	<0.3	<2	1	1	5	<5	0.030
485715	886	<3	198	<0.3	<2	1	8	74	<5	0.518
485716	183	4	20	<0.3	<2	2	6	11	<5	0.038
485717	1068	4	24	<0.3	<2	1	36	16	36	0.137
485718	217	13	8	<0.3	<2	1	5	7	5	0.033
485719	123	6	46	<0.3	<2	3	63	33	80	1.680
485720	36	8	30	<0.3	<2	2	8	6	133	0.518
485721	8	9	9	<0.3	<2	2	12	6	12	2.500

GGU no.	Cu ppm	Pb ppm	Zn ppm	Cd ppm	Bi ppm	Mo ppm	Ni ppm	Co ppm	Cr ppm	S pct
485722	74	<3	95	<0.3	<2	7	67	21	40	1.917
485723	152	<3	59	<0.3	5	5	41	11	25	0.987
485724	30	<3	35	<0.3	2	2	23	8	36	0.634
485725	30	<3	39	<0.3	3	5	26	13	18	0.522
485726	4223	8	4	<0.3	<2	2	9	7	7	0.114
485727	17	4	3	<0.3	<2	6	7	17	<5	3.401
485728	11	<3	4	<0.3	<2	2	4	7	<5	0.479
485729	68	<3	361	0.8	3	5	98	16	15	2.527
485730	23	<3	288	<0.3	8	4	6	5	14	0.319
485731	20	5	337	<0.3	6	4	5	7	17	0.201
485732	15	<3	90	<0.3	5	4	47	5	39	0.081
485733	17	<3	114	<0.3	5	5	41	6	35	0.069
485734	14	<3	111	<0.3	6	5	27	4	<5	0.038
485735	261	6	121	<0.3	<2	1	176	106	238	0.185
485736	10	<3	22	<0.3	<2	2	8	6	24	0.296
485737	8	<3	46	<0.3	<2	2	15	7	35	0.051
485738	15	4	48	<0.3	<2	<1	6	8	18	0.536
485739	47	9	85	<0.3	<2	3	13	48	<5	0.323
485740	9	8	114	<0.3	<2	3	4	12	10	0.006
485741	368	4	78	<0.3	<2	9	297	60	73	2.575
485742	38	9	58	<0.3	2	4	39	16	148	0.244
485743	123	<3	91	<0.3	6	7	50	19	60	2.618
485744	133	<3	113	<0.3	2	7	73	24	125	1.593
485745	129	5	92	<0.3	<2	5	69	25	29	1.689
485746	80	4	86	<0.3	<2	3	32	18	127	1.022
485747	54	<3	47	<0.3	2	4	30	13	45	0.820
485748	213	14	80	<0.3	<2	3	66	19	184	0.290
485749	83	15	51	<0.3	<2	2	32	21	83	0.100
485750	92	17	64	<0.3	<2	4	65	18	151	0.038
485751	146	<3	100	<0.3	4	7	55	19	74	1.651
485752	64	<3	123	<0.3	2	5	34	12	48	1.015
485753	25	4	94	<0.3	7	6	25	13	62	0.225
485754	137	<3	85	<0.3	3	7	56	19	70	1.609
485755	238	6	53	<0.3	<2	3	35	37	134	0.758
485756	340	4	41	<0.3	<2	8	178	40	29	2.820
485757	19	7	75	<0.3	<2	2	10	16	29	0.198
485758	88	13	65	<0.3	<2	2	22	16	17	1.653
485759	48	11	60	<0.3	<2	1	44	16	176	1.477
485760	229	15	793	<0.3	<2	82	117	79	164	2.050
485761	19	8	160	<0.3	<2	3	7	5	222	0.053
485762	213	135	51	<0.3	5	116	581	151	90	16.522
485763	9	17	3	<0.3	<2	2	19	6	7	10.881
485764	11	11	<1	<0.3	3	1	33	11	<5	12.352
485765	20	56	1	<0.3	5	3	167	39	13	18.213

GGU no.	Cu ppm	Pb ppm	Zn ppm	Cd ppm	Bi ppm	Mo ppm	Ni ppm	Co ppm	Cr ppm	S pct
485766	44	<3	25	<0.3	<2	5	13	9	21	0.337
485767	285	<3	75	<0.3	<2	4	72	49	184	1.934
485768	338	<3	219	<0.3	<2	1	4	40	14	1.569
485769	70	<3	52	<0.3	4	5	22	12	34	0.539
485770	60	4	47	<0.3	<2	3	15	5	9	0.860
485771	37	<3	46	<0.3	5	5	19	9	57	0.408
485772	160	44	60	<0.3	<2	40	94	35	65	4.419
485773	166	21	637	1.6	<2	3	33	14	68	3.839
485774	15	11	60	<0.3	<2	2	7	17	35	0.238
485775	48	<3	85	<0.3	<2	<1	83	37	176	0.117
485776	90	9	149	<0.3	<2	2	79	35	211	0.618
485777	700	171	84	<0.3	<2	11	11	6	100	0.351
485778	42	10	46	<0.3	<2	4	9	30	18	0.469
485779	62	<3	173	<0.3	<2	<1	97	49	270	0.727
485780	91	7	116	<0.3	<2	1	81	75	118	0.635
485781	133	28	151	<0.3	<2	11	144	48	293	0.582
485782	168	19	106	<0.3	<2	7	90	48	241	0.988
485783	144	10	5	<0.3	<2	2	4	4	14	0.355
485784	665	11	8	<0.3	<2	<1	3	17	14	0.083
485785	63	<3	7	<0.3	<2	3	35	20	61	0.472
485786	21	114	20986	15.6	<2	<1	26	56	39	1.441
485787	58	28	247	<0.3	<2	2	43	60	65	1.814
485788	212	10	76	<0.3	<2	4	44	67	75	4.460
485789	26	12	16	<0.3	<2	1	10	8	30	1.741
485790	130	157	461	<0.3	<2	<1	9	16	22	1.073
485791	>99999	2046	25	<0.3	4	47	17	9	15	0.430
485792	30	<3	36	<0.3	<2	2	71	25	280	0.007
485793	41	<3	30	<0.3	<2	3	58	25	210	0.010
485794	1362	5	22	<0.3	<2	2	44	58	145	0.016
485795	10167	12	46	<0.3	<2	2	103	86	177	0.180
485796	479	6	60	<0.3	<2	1	119	56	273	0.009
485797	81	<3	151	<0.3	<2	<1	43	40	46	0.253
485798	101	<3	55	<0.3	<2	1	1134	105	2000	0.665
485799	86	4	120	<0.3	<2	4	47	49	48	0.274
485800	38	<3	182	<0.3	<2	3	100	42	187	0.107
485801	619	<3	144	<0.3	<2	6	1297	167	2850	2.113
485802	513	21	47	<0.3	<2	5	35	41	16	1.241
485803	1047	37	53	<0.3	<2	7	43	77	44	2.333
485804	12	8	3	<0.3	<2	4	7	2	7	2.220
485805	678	10	117	<0.3	<2	6	1186	174	1420	3.150
485806	1089	<3	112	<0.3	<2	4	652	106	2220	4.219
485807	806	<3	112	<0.3	<2	3	1073	151	1270	3.420
485808	241	9	112	<0.3	<2	5	52	24	88	1.735
485809	1748	<3	127	<0.3	<2	4	406	150	25	5.438

GGU no.	Cu ppm	Pb ppm	Zn ppm	Cd ppm	Bi ppm	Mo ppm	Ni ppm	Co ppm	Cr ppm	S pct
485810	1403	<3	149	<0.3	<2	4	704	239	54	8.211
485811	518	12	215	0.5	2	9	339	113	98	10.150
485812	611	6	235	<0.3	<2	6	25	20	32	2.841
485813	688	17	152	<0.3	<2	9	34	20	29	4.263
485814	90	16	94	<0.3	<2	7	96	34	100	0.336
485815	20	1	72	<0.3	2	5	24	11	49	0.197
485816	1315	31	59	<0.3	<2	22	348	185	117	6.320
485817	587	16	223	<0.3	<2	9	78	82	53	2.055
485818	113	11	123	<0.3	<2	5	86	20	318	0.483
485819	300	<3	165	0.6	<2	7	13	16	18	1.314
485820	186	<3	89	0.6	<2	8	23	13	31	1.293
485821	121	<3	75	0.4	<2	6	5	8	19	0.610
485822	49	45	188	<0.3	<2	2	16	13	35	0.236
485823	818	7	136	0.4	<2	7	384	108	101	1.207
485824	1632	7	173	<0.3	5	4	386	115	498	1.739
485825	924	<3	99	<0.3	<2	<1	659	124	556	2.218
485826	941	<3	116	<0.3	<2	17	950	159	72	6.842
485827	527	<3	100	0.3	<2	7	121	70	115	4.454
485828	44	<3	26	<0.3	<2	2	56	17	71	0.227
485829	1396	3	77	0.0	<2	24	1289	91	671	7.485
485830	1116	12	5	<0.3	<2	<1	7	5	50	0.030
485831	119	13	46	<0.3	<2	2	34	21	91	0.039
Samples	152	152	152	152	152	152	152	152	152	152
Minimum	7	<3	<1	<0.3	<2	<1	1	<1	<5	0.006
Maximum	>99999	2046	20986	15.6	8	1213	3582	239	3250	18.213
Median	133	6	77	<0.3	<2	4	44	23	61	0.988

GGU no.	W ppm	Ta ppm	Sn pct	Be ppm	Br ppm	Rb ppm	Sr ppm	Sc ppm	Cs ppm	Hf ppm	Y ppm
470001	3	<0.5	<0.01	1	<0.5	<15	607	14.0	<1	2	10
470002	<1	<0.5	<0.01	<1	0.6	24	20	1.4	<1	1	5
470003	5	5.4	<0.01	<1	<0.5	26	11	48.9	<1	12	30
470004	<1	<0.5	<0.01	1	<0.5	<15	330	27.4	<1	2	12
470005	<1	1.1	<0.01	4	<0.5	178	330	16.8	<1	6	17
470006	<1	<0.5	<0.01	1	<0.5	150	294	7.0	<1	10	<1
470007	3	3.3	<0.01	<1	<0.5	45	312	16.4	1	3	40
470008	<1	2.0	<0.01	<1	<0.5	38	158	10.5	<1	8	13
470009	<1	1.6	<0.01	2	<0.5	37	958	26.0	<1	7	48
470010	<1	<0.5	<0.01	<1	<0.5	33	103	31.7	1	1	9
470020	7	0.6	<0.01	2	<0.5	<15	189	13.3	2	2	13
470021	<1	0.6	<0.01	<1	<0.5	<15	121	16.5	<1	1	27
470022	<1	<0.5	<0.01	3	<0.5	<15	46	2.2	<1	<1	10
470023	<1	<0.5	<0.01	2	<0.5	98	185	24.4	9	2	26
470024	<1	<0.5	<0.01	<1	<0.5	39	57	5.4	1	5	10
470025	<1	<0.5	<0.01	2	<0.5	105	146	0.9	2	4	2
470026	<1	1.6	<0.01	2	<0.5	<15	119	45.9	<1	12	34
470027	<1	<0.5	<0.01	<1	<0.5	<15	26	3.5	<1	3	7
470028	3	<0.5	<0.01	<1	2.2	<15	32	5.8	<1	1	19
470029	<1	<0.5	<0.01	2	<0.5	60	258	25.1	<1	1	15
470030	<1	<0.5	<0.01	<1	1.6	38	76	1.5	<1	2	9
485701	<1	<0.5	<0.01	2	<0.5	30	175	8.1	<1	11	6
485702	<1	<0.5	<0.01	<1	<0.5	46	230	9.5	<1	6	7
485703	<1	<0.5	<0.01	2	<0.5	82	256	1.4	<1	8	2
485704	<1	<0.5	<0.01	2	<0.5	37	520	1.6	<1	2	1
485705	<1	1.0	<0.01	1	<0.5	<15	260	22.9	1	13	18
485706	<1	0.7	<0.01	1	<0.5	60	343	21.2	<1	3	6
485707	<1	<0.5	<0.01	<1	16.4	<15	28	0.2	<1	<1	5
485708	<1	<0.5	<0.01	<1	<0.5	<15	10	24.2	<1	2	134
485709	<1	0.7	<0.01	<1	<0.5	<15	3	3.2	<1	<1	7
485710	<1	<0.5	<0.01	<1	<0.5	<15	14	26.5	<1	<1	52
485711	29	<0.5	<0.01	<1	0.9	<15	21	0.3	<1	2	2
485712	16	<0.5	<0.01	<1	1.4	19	135	1.7	<1	3	6
485713	<1	<0.5	<0.01	<1	0.7	<15	156	0.3	<1	2	2
485714	<1	<0.5	<0.01	<1	1.1	19	16	0.3	<1	1	3
485715	<1	1.8	<0.01	<1	<0.5	<15	28	55.5	<1	3	103
485716	46	<0.5	<0.01	<1	<0.5	60	1	0.2	<1	<1	3
485717	<1	<0.5	<0.01	2	7.0	90	18	5.5	1	<1	78
485718	26	1.0	<0.01	1	9.0	93	10	1.5	1	<1	13
485719	<1	<0.5	<0.01	1	1.8	91	46	7.0	2	1	2
485720	<1	<0.5	<0.01	<1	<0.5	54	34	9.1	1	3	9
485721	15	<0.5	<0.01	<1	<0.5	20	34	2.6	<1	1	4

GGU no.	W ppm	Ta ppm	Sn pct	Be ppm	Br ppm	Rb ppm	Sr ppm	Sc ppm	Cs ppm	Hf ppm	Y ppm
485722	<1	<0.5	<0.01	1	<0.5	<15	27	6.6	1	<1	14
485723	<1	<0.5	<0.01	1	<0.5	<15	34	4.9	<1	<1	18
485724	<1	<0.5	<0.01	2	<0.5	<15	121	4.2	<1	<1	16
485725	4	<0.5	<0.01	<1	<0.5	<15	52	2.5	2	<1	4
485726	12	<0.5	<0.01	<1	<0.5	48	88	0.7	<1	2	3
485727	<1	<0.5	<0.01	<1	<0.5	<15	81	1.2	<1	2	8
485728	3	<0.5	<0.01	<1	<0.5	<15	104	1.1	<1	2	6
485729	2	<0.5	<0.01	<1	<0.5	<15	6	3.4	<1	<1	11
485730	<1	<0.5	<0.01	<1	<0.5	<15	7	3.8	<1	<1	10
485731	19	<0.5	<0.01	<1	<0.5	<15	10	2.3	<1	<1	7
485732	<1	<0.5	<0.01	1	<0.5	<15	8	1.8	<1	<1	10
485733	<1	<0.5	<0.01	<1	<0.5	<15	5	1.3	<1	<1	4
485734	<1	<0.5	<0.01	<1	<0.5	<15	4	1.3	<1	<1	7
485735	<1	<0.5	<0.02	2	<0.5	42	258	46.2	3	2	22
485736	<1	<0.5	<0.01	1	<0.5	77	16	3.1	<1	2	6
485737	<1	<0.5	<0.01	<1	<0.5	46	13	4.8	<1	2	4
485738	<1	<0.5	<0.01	2	<0.5	177	10	6.2	<1	8	5
485739	<1	<0.5	<0.03	<1	<0.5	<15	497	33.8	<1	2	16
485740	<1	1.4	<0.02	2	<0.5	106	273	16.4	1	13	23
485741	<1	0.7	<0.02	<1	<0.5	<15	78	8.8	<1	2	13
485742	<1	0.6	<0.02	1	<0.5	<15	158	13.9	1	2	10
485743	<1	<0.5	<0.02	<1	<0.5	<15	34	11.1	2	2	17
485744	<1	<0.5	<0.01	<1	<0.5	<15	22	14.9	<1	<1	23
485745	2	<0.5	<0.01	3	<0.5	<15	145	3.9	<1	<1	10
485746	<1	<0.5	<0.01	<1	<0.5	<15	100	12.6	<1	1	24
485747	<1	<0.5	<0.01	2	<0.5	<15	37	6.4	<1	<1	23
485748	<1	<0.5	<0.02	1	<0.5	152	284	14.3	<1	4	13
485749	<1	<0.5	<0.02	2	<0.5	70	209	8.6	1	4	12
485750	<1	<0.5	<0.02	3	<0.5	80	219	11.6	<1	4	8
485751	3	<0.5	<0.01	<1	<0.5	<15	57	10.1	<1	1	25
485752	<1	<0.5	<0.01	<1	<0.5	<15	11	6.7	1	<1	9
485753	7	<0.5	<0.01	<1	<0.5	<15	55	9.8	<1	1	27
485754	4	<0.5	<0.01	1	1.4	30	82	9.4	1	1	20
485755	<1	0.8	<0.02	<1	<0.5	<15	252	40.5	<1	5	25
485756	<1	<0.5	<0.01	2	<0.5	<15	130	5.0	<1	2	8
485757	<1	<0.5	<0.01	2	<0.5	91	518	13.6	<1	7	14
485758	<1	<0.5	<0.01	<1	<0.5	<15	5	3.5	<1	2	7
485759	<1	0.7	<0.01	<1	0.3	86	51	14.9	<1	5	17
485760	<1	1.0	<0.01	<1	<0.5	<15	219	30.8	<1	26	42
485761	<1	<0.5	<0.01	<1	<0.5	120	24	9.5	4	8	<1
485762	7	0.8	<0.02	<1	2.2	69	13	11.7	3	2	21
485763	<1	<0.5	<0.01	<1	<0.5	<15	53	0.4	<1	<1	<1
485764	<1	<0.5	<0.01	<1	1.4	<15	1	0.3	<1	<1	<1
485765	<1	<0.5	<0.01	<1	<0.5	<15	5	0.3	<1	<1	<1

GGU no.	W ppm	Ta ppm	Sn pct	Be ppm	Br ppm	Rb ppm	Sr ppm	Sc ppm	Cs ppm	Hf ppm	Y ppm
485766	<1	<0.5	<0.01	3	<0.5	<15	66	1.8	<1	<1	9
485767	<1	1.1	<0.02	2	<0.5	<15	275	40.8	3	4	35
485768	<1	2.6	<0.02	2	<0.5	<15	96	52.7	2	9	108
485769	<1	<0.5	<0.02	2	<0.5	<15	23	14.0	<1	<1	93
485770	<1	<0.5	<0.01	2	<0.5	<15	37	1.5	<1	<1	7
485771	2	1.1	<0.01	2	<0.5	<15	29	6.3	<1	<1	24
485772	<1	1.1	<0.01	<1	<0.5	91	66	6.7	2	2	3
485773	<1	<0.5	<0.01	3	2.0	<15	29	6.7	1	3	5
485774	<1	0.9	<0.02	2	<0.5	83	246	19.2	<1	11	16
485775	<1	<0.5	<0.01	<1	<0.5	<15	192	22.6	<1	3	30
485776	<1	2.2	<0.02	2	<0.5	93	911	29.0	<1	5	89
485777	<1	<0.5	<0.01	3	<0.5	99	203	1.3	1	10	3
485778	<1	1.0	<0.01	2	2.4	106	1219	33.8	2	5	23
485779	<1	0.9	<0.01	2	<0.5	87	1733	27.1	<1	5	46
485780	<1	<0.5	<0.01	2	<0.5	<15	956	46.3	<1	4	38
485781	<1	<0.5	<0.01	2	<0.5	<15	147	80.7	<1	17	139
485782	<1	1.4	<0.02	4	<0.5	67	252	49.0	<1	8	71
485783	<1	<0.5	<0.01	<1	1.3	<15	12	0.8	<1	3	3
485784	<1	<0.5	<0.01	<1	1.9	<15	5	0.7	<1	2	3
485785	<1	1.2	<0.02	2	<0.5	<15	51	14.0	3	6	25
485786	<1	0.8	<0.02	2	<0.5	<15	114	5.8	2	2	19
485787	<1	0.8	<0.02	2	<0.5	95	95	12.2	3	3	16
485788	<1	<0.5	<0.02	3	<0.5	89	57	16.1	<1	4	42
485789	<1	<0.5	<0.01	<1	<0.5	<15	55	4.6	<1	3	5
485790	<1	<0.5	<0.01	<1	1.8	<15	332	3.7	<1	<1	9
485791	<1	<0.5	<0.02	<1	<0.5	63	129	1.8	<1	2	11
485792	<1	1.1	<0.02	<1	<0.5	<15	317	31.5	<1	4	26
485793	<1	0.6	<0.02	<1	<0.5	40	195	24.8	<1	2	27
485794	<1	<0.5	<0.01	<1	2.0	60	86	13.7	<1	7	16
485795	<1	<0.5	<0.01	4	<0.5	41	81	30.6	<1	5	26
485796	7	<0.5	<0.02	<1	2.5	74	222	46.2	<1	1	25
485797	<1	<0.5	<0.01	<1	<0.5	47	147	53.1	<1	2	25
485798	<1	<0.5	<0.01	<1	<0.5	<15	115	21.4	<1	<1	12
485799	<1	1.4	<0.02	3	<0.5	72	463	54.1	<1	4	104
485800	<1	2.2	<0.02	3	<0.5	70	163	62.3	2	9	116
485801	<1	<0.5	<0.01	<1	<0.5	<15	57	41.1	2	1	25
485802	<1	<0.5	<0.01	1	<0.5	80	296	2.4	<1	4	<1
485803	<1	<0.5	<0.02	<1	<0.5	35	141	10.1	<1	3	9
485804	<1	<0.5	<0.01	<1	1.5	<15	8	0.4	<1	<1	2
485805	4	2.7	<0.02	2	<0.5	<15	337	35.5	<1	4	35
485806	<1	1.1	<0.01	1	<0.5	<15	124	36.2	<1	2	17
485807	<1	1.8	<0.01	1	<0.5	<15	192	33.6	<1	2	21
485808	<1	<0.5	<0.01	<1	<0.5	<15	184	11.9	<1	2	17
485809	<1	0.6	<0.01	<1	<0.5	<15	16	40.9	<1	1	39

GGU no.	W ppm	Ta ppm	Sn pct	Be ppm	Br ppm	Rb ppm	Sr ppm	Sc ppm	Cs ppm	Hf ppm	Y ppm
485810	<1	<0.5	<0.02	1	<0.5	76	20	45.2	<1	<1	45
485811	<1	0.8	<0.01	1	<0.5	147	38	13.6	2	2	15
485812	<1	2.4	<0.02	2	<0.5	76	98	17.9	6	14	29
485813	<1	2.5	<0.01	1	<0.5	111	72	12.2	5	14	32
485814	<1	<0.5	<0.02	3	<0.5	88	464	27.3	2	2	30
485815	<1	1.2	<0.01	5	<0.5	<15	82	13.5	<1	1	16
485816	7	1.6	<0.01	3	<0.5	204	116	11.2	3	3	8
485817	<1	0.9	<0.01	1	<0.5	123	348	27.8	10	1	19
485818	<1	<0.5	<0.01	2	<0.5	226	49	11.9	5	2	35
485819	<1	<0.5	<0.01	<1	<0.5	28	5	2.5	<1	<1	15
485820	<1	<0.5	<0.01	<1	<0.5	<15	16	5.2	<1	<1	21
485821	<1	<0.5	<0.01	<1	<0.5	<15	5	2.6	<1	<1	11
485822	<1	0.9	<0.02	4	<0.5	159	243	7.6	5	5	13
485823	<1	<0.5	<0.01	<1	<0.5	<15	31	19.9	<1	<1	17
485824	<1	<0.5	<0.01	<1	<0.5	<15	66	29.5	<1	<1	15
485825	<1	1.8	<0.01	2	<0.5	<15	180	20.0	<1	1	14
485826	<1	0.7	<0.01	<1	<0.5	113	170	11.8	3	3	8
485827	<1	0.7	<0.01	<1	<0.5	42	54	10.4	<1	2	9
485828	<1	<0.5	<0.01	<1	1.5	30	65	5.3	<1	<1	2
485829	<1	0.7	<0.01	1	<0.5	84	280	16.0	4	2	13
485830	9	1.3	<0.01	<1	1.5	110	151	7.8	2	28	30
485831	4	1.7	<0.01	3	1.9	205	463	14.8	7	14	60
Samples	152	152	152	152	152	152	152	152	152	152	152
Minimum	<1	<0.5	<0.03	<1	<0.5	<15	1	0.2	<1	<1	<1
Maximum	46	5.4	<0.01	5	16.4	226	1733	80.7	10	28	139
Median	<1	<0.5	<0.01	<1	<0.5	<15	87	10.5	<1	2	14

GGU no.	U ppm	Th ppm	La ppm	Ce ppm	Nd ppm	Sm ppm	Eu ppm	Tb ppm	Yb ppm	Lu ppm	Ba ppm
470001	<0.5	3.8	68.0	95	26	4.0	3.0	<0.5	3.2	0.48	2000
470002	0.9	0.9	2.6	5	<5	0.5	<0.2	<0.5	0.4	0.06	210
470003	1.7	2.3	9.8	19	<5	4.1	<0.2	2.0	3.4	0.36	<50
470004	<0.5	<0.2	12.4	24	14	3.1	0.7	<0.5	1.0	0.15	360
470005	3.0	39.2	79.4	140	45	8.3	1.5	<0.5	0.8	0.13	1800
470006	<0.5	<0.2	30.0	45	12	1.0	1.3	<0.5	0.5	0.08	740
470007	2.0	1.8	35.6	60	17	3.4	1.5	<0.5	2.5	0.37	710
470008	<0.5	1.5	32.6	53	13	3.6	1.2	0.9	1.8	0.27	330
470009	<0.5	2.1	28.1	71	41	11.8	3.5	1.6	2.8	0.44	270
470010	<0.5	<0.2	5.8	13	<5	2.0	0.4	<0.5	0.8	0.12	270
470020	2.2	6.2	14.4	28	12	2.9	0.9	<0.5	1.3	0.20	190
470021	1.8	4.1	8.5	16	6	2.5	1.1	0.6	1.8	0.26	77
470022	1.3	0.8	6.8	14	5	1.1	0.6	<0.5	0.8	0.13	<50
470023	1.1	2.3	19.7	47	23	5.7	1.1	0.8	1.8	0.27	230
470024	1.5	7.8	22.1	42	13	3.2	1.0	<0.5	1.1	0.17	430
470025	0.6	1.2	7.4	12	5	0.8	1.4	<0.5	0.3	0.05	940
470026	1.1	5.8	29.6	50	12	7.4	0.9	1.6	2.3	0.35	470
470027	1.1	4.2	12.4	23	10	2.3	0.6	<0.5	1.0	0.15	320
470028	<0.5	4.4	54.6	108	45	9.6	1.6	<0.5	1.3	0.20	<50
470029	<0.5	1.9	12.5	26	13	3.2	1.0	<0.5	1.4	0.22	290
470030	0.8	3.6	8.0	20	9	2.0	0.4	<0.5	0.5	0.07	210
485701	<0.5	24.8	76.5	141	47	7.2	1.2	<0.5	0.8	0.12	420
485702	<0.5	5.8	62.1	113	38	6.9	1.6	<0.5	1.0	0.15	580
485703	<0.5	17.5	81.9	140	50	7.9	2.1	<0.5	0.5	0.07	1800
485704	<0.5	24.9	76.5	134	49	6.7	2.1	<0.5	<0.2	<0.05	470
485705	1.1	2.7	45.5	70	21	4.3	1.4	0.9	4.0	0.60	460
485706	1.2	7.6	37.9	65	24	4.8	1.6	<0.5	1.2	0.18	980
485707	<0.5	0.2	9.9	15	6	1.1	0.4	<0.5	0.2	<0.05	<50
485708	<0.5	66.6	179.0	341	115	16.0	0.5	2.0	24.0	3.66	<50
485709	<0.5	22.8	47.4	90	32	6.1	0.3	<0.5	0.5	0.08	<50
485710	<0.5	17.9	89.4	153	51	10.0	0.6	1.5	3.0	0.45	<50
485711	0.6	3.1	5.9	12	<5	0.7	<0.2	<0.5	0.3	<0.05	<50
485712	1.2	2.5	12.1	32	12	2.6	0.5	<0.5	0.5	0.07	150
485713	<0.5	2.5	6.2	15	<5	0.6	<0.2	<0.5	0.2	<0.05	8300
485714	<0.5	1.7	19.6	41	15	2.5	0.3	<0.5	0.2	<0.05	190
485715	1.1	1.7	17.8	49	31	10.6	2.2	2.9	8.4	1.27	<50
485716	2.3	2.2	6.4	11	6	0.9	<0.2	<0.5	<0.2	<0.05	<50
485717	2.0	3.9	132.0	304	131	26.5	6.8	3.0	6.6	0.98	170
485718	4.6	9.4	5.0	11	<5	1.8	0.3	<0.5	1.2	0.18	120
485719	<0.5	2.9	4.4	11	<5	1.0	0.3	<0.5	0.4	0.06	270
485720	1.2	8.9	26.7	50	19	3.7	0.7	<0.5	1.2	0.19	300
485721	<0.5	5.1	14.8	28	8	1.9	0.5	<0.5	0.4	0.07	400

GGU no.	U ppm	Th ppm	La ppm	Ce ppm	Nd ppm	Sm ppm	Eu ppm	Tb ppm	Yb ppm	Lu ppm	Ba ppm
485722	1.3	1.8	10.2	21	11	2.5	0.7	<0.5	1.2	0.17	240
485723	1.0	3.7	16.6	33	11	2.2	0.7	<0.5	2.3	0.35	<50
485724	<0.5	1.0	9.1	19	8	2.2	0.7	<0.5	1.2	0.20	<50
485725	<0.5	1.1	2.6	6	<5	0.6	0.3	<0.5	0.5	0.07	<50
485726	1.1	3.1	9.4	20	7	1.2	0.3	<0.5	0.5	0.08	2800
485727	<0.5	2.4	26.8	55	22	5.7	1.0	<0.5	0.6	0.10	5500
485728	<0.5	2.1	44.7	69	29	3.5	0.8	<0.5	0.6	0.10	5500
485729	<0.5	<0.2	1.0	4	<5	0.4	0.3	<0.5	0.8	0.12	225
485730	<0.5	<0.2	1.9	<3	<5	0.8	0.5	<0.5	1.0	0.16	<50
485731	<0.5	<0.2	1.1	<3	<5	0.5	0.3	<0.5	0.7	0.11	<50
485732	<0.5	<0.2	4.0	8	<5	0.9	0.4	<0.5	0.6	0.10	<50
485733	<0.5	0.9	3.8	8	<5	0.7	0.3	<0.5	<0.2	<0.05	<50
485734	<0.5	<0.2	4.1	7	<5	0.7	0.3	<0.5	0.7	0.11	<50
485735	<0.5	9.4	15.5	36	15	5.3	1.1	<0.5	1.3	0.21	410
485736	<0.5	6.3	28.3	62	21	4.1	0.6	<0.5	<0.2	<0.05	290
485737	<0.5	7.9	18.9	38	22	2.8	0.5	<0.5	0.2	<0.05	280
485738	<0.5	10.7	39.4	66	22	4.3	0.7	0.6	1.2	0.20	620
485739	<0.5	<0.2	18.0	39	21	5.3	2.6	<0.5	2.7	0.41	2000
485740	<0.5	1.9	37.9	73	35	7.8	2.7	1.2	3.5	0.53	2200
485741	2.1	6.6	19.6	29	8	3.3	0.5	0.6	1.2	0.17	270
485742	<0.5	1.3	17.4	29	11	2.8	0.9	0.5	1.1	0.16	210
485743	1.9	3.6	12.9	23	6	3.2	1.3	0.6	1.5	0.23	<50
485744	<0.5	<0.2	6.2	12	<5	2.6	0.6	0.5	2.0	0.31	<50
485745	<0.5	1.3	11.8	21	<5	2.0	0.9	0.6	0.8	0.14	<50
485746	<0.5	0.6	8.6	20	<5	2.7	0.8	<0.5	3.0	0.45	<50
485747	<0.5	<0.2	8.8	18	8	1.9	0.9	<0.5	1.1	0.14	<50
485748	1.5	8.4	32.5	51	17	3.8	1.0	0.6	1.5	0.22	980
485749	<0.5	1.3	11.8	16	<5	1.2	0.7	<0.5	2.1	0.31	560
485750	1.9	6.0	30.0	45	11	3.1	0.9	1.0	1.3	0.19	740
485751	<0.5	1.2	12.6	23	13	3.2	1.1	<0.5	1.8	0.25	<50
485752	<0.5	0.6	5.4	11	<5	1.5	0.6	<0.5	0.8	0.13	<50
485753	<0.5	2.1	5.1	12	<5	3.3	1.0	<0.5	2.0	0.32	330
485754	<0.5	<0.2	11.5	20	13	2.9	1.1	<0.5	1.6	0.24	<50
485755	1.5	1.7	10.3	25	13	3.9	0.9	<0.5	3.3	0.50	<55
485756	4.1	7.9	12.8	25	6	2.5	0.7	<0.5	0.9	0.16	<50
485757	<0.5	2.7	56.9	96	52	8.6	2.2	<0.5	1.1	0.16	1900
485758	1.6	3.7	6.2	10	<5	1.1	<0.2	<0.5	0.5	0.09	<50
485759	1.5	14.4	36.3	63	21	4.5	1.1	0.1	3.0	0.46	465
485760	1.9	43.5	126.0	203	70	12.1	2.1	<0.5	5.9	0.79	230
485761	1.1	4.2	7.7	12	<5	0.8	0.6	<0.5	0.4	0.06	460
485762	9.3	8.0	25.3	41	15	3.4	1.0	<0.5	1.8	0.26	<50
485763	<0.5	<0.2	4.3	8	<5	0.3	0.4	<0.5	<0.2	<0.05	2400
485764	<0.5	1.1	3.0	4	<5	0.3	<0.2	<0.5	<0.2	<0.05	<50
485765	<0.5	0.8	3.5	<3	<5	0.4	<0.2	<0.5	<0.2	<0.05	<50

GGU no.	U ppm	Th ppm	La ppm	Ce ppm	Nd ppm	Sm ppm	Eu ppm	Tb ppm	Yb ppm	Lu ppm	Ba ppm
485766	<0.5	1.2	7.4	12	<5	1.2	0.5	<0.5	0.8	0.12	<50
485767	<0.5	2.2	21.1	46	14	6.5	2.0	<0.5	3.3	0.50	<50
485768	<0.5	2.7	41.7	93	45	17.1	5.4	3.6	11.9	1.68	510
485769	1.9	17.1	30.1	65	22	6.0	0.7	1.3	12.0	1.79	<50
485770	0.7	0.7	5.5	10	5	1.1	0.5	<0.5	0.5	0.07	<50
485771	1.5	10.0	21.9	42	16	4.1	0.8	<0.5	1.8	0.26	<50
485772	1.7	12.1	31.0	47	17	3.5	1.5	<0.5	0.4	0.06	800
485773	1.6	7.4	6.0	12	5	1.0	0.7	<0.5	0.6	0.09	<50
485774	<0.5	9.6	61.2	121	50	13.3	1.8	0.9	2.5	0.36	1500
485775	<0.5	<0.2	10.8	24	13	3.8	1.2	0.9	2.6	0.35	<50
485776	1.9	13.1	97.3	225	105	26.3	5.3	2.6	6.1	0.91	1500
485777	<0.5	3.0	19.2	28	9	1.6	1.6	<0.5	0.9	0.14	2200
485778	<0.5	10.1	114.0	224	100	18.6	3.1	1.1	1.6	0.24	2600
485779	<0.5	5.4	116.0	240	110	22.4	5.4	1.3	2.8	0.42	940
485780	<0.5	4.6	75.1	151	77	21.6	5.6	2.0	2.0	0.30	1500
485781	1.8	133.0	131.0	242	81	17.5	1.4	4.3	16.1	2.41	<75
485782	1.4	3.8	47.2	74	20	6.1	2.0	1.5	7.4	1.16	1200
485783	0.7	1.9	16.0	30	8	2.0	0.4	<0.5	0.3	<0.05	320
485784	1.5	1.5	8.5	18	7	1.4	0.3	<0.5	0.4	0.06	390
485785	3.5	13.1	61.3	119	52	14.0	2.7	<0.5	3.2	0.47	320
485786	1.2	4.5	24.5	51	20	6.2	1.1	<0.5	1.2	0.19	<50
485787	1.5	9.8	34.1	57	22	4.7	0.8	<0.5	1.6	0.25	520
485788	3.2	14.7	72.4	136	59	20.6	3.7	3.9	4.2	0.61	820
485789	1.2	4.7	14.2	26	10	1.7	0.3	<0.5	0.7	0.11	285
485790	<0.5	2.0	18.2	27	12	3.2	0.5	<0.5	0.7	0.11	120
485791	13.3	<0.2	41.3	72	24	4.1	4.5	<0.5	0.5	0.08	14000
485792	1.6	2.2	33.6	55	20	4.9	1.8	<0.5	2.6	0.37	2500
485793	<0.5	2.2	159.0	225	76	11.3	3.5	<0.5	2.3	0.31	500
485794	5.1	5.9	11.3	25	7	2.8	1.0	<0.5	1.8	0.26	1500
485795	5.9	3.1	9.2	16	11	2.2	0.6	<0.5	2.7	0.41	8600
485796	1.0	<0.2	5.2	14	<5	2.9	1.1	<0.5	2.4	0.35	1600
485797	1.0	<0.2	7.3	17	5	2.5	0.9	<0.5	2.5	0.38	210
485798	<0.5	<0.2	5.5	10	<5	0.9	0.5	<0.5	0.9	0.14	<50
485799	<0.5	2.8	61.3	159	86	25.0	2.5	3.6	7.0	1.10	600
485800	2.9	7.4	92.6	232	120	31.7	3.5	3.2	7.3	1.15	600
485801	<0.5	<0.2	2.9	9	<5	1.7	0.6	<0.5	2.1	0.33	<50
485802	1.1	4.5	19.1	28	<5	0.9	1.0	<0.5	<0.2	<0.05	1400
485803	3.0	1.1	13.9	25	<5	1.6	0.6	<0.5	1.2	0.08	200
485804	<0.5	1.2	3.6	9	<5	0.5	<0.2	<0.5	0.2	<0.05	57
485805	7.4	9.8	49.4	93	39	9.6	2.6	1.4	3.0	0.44	290
485806	<0.5	1.8	16.7	32	12	3.9	1.3	<0.5	1.5	0.22	<50
485807	2.1	4.0	33.5	52	21	5.3	1.8	<0.5	1.8	0.26	770
485808	1.4	2.8	20.6	33	9	2.4	0.8	<0.5	1.7	0.27	300
485809	<0.5	3.8	14.6	41	26	10.2	0.9	1.3	3.3	0.49	300

GGU no.	U ppm	Th ppm	La ppm	Ce ppm	Nd ppm	Sm ppm	Eu ppm	Tb ppm	Yb ppm	Lu ppm	Ba ppm
485810	2.0	12.6	33.2	87	46	13.3	1.0	1.7	3.5	0.53	400
485811	3.7	7.4	18.3	29	7	2.8	0.8	<0.5	1.4	0.21	470
485812	2.5	16.0	50.7	101	38	15.2	3.4	3.4	13.9	2.00	1700
485813	2.5	14.7	57.4	114	44	15.4	3.1	3.0	13.6	1.98	1200
485814	1.6	<0.2	12.0	24	7	4.6	1.2	0.9	3.2	0.48	450
485815	1.4	<0.2	13.1	25	7	3.0	2.1	<0.5	1.6	0.24	260
485816	11.2	17.1	18.2	28	6	2.3	<0.2	<0.5	0.9	0.16	430
485817	3.2	1.5	10.0	22	15	3.5	2.5	<0.5	1.6	0.24	780
485818	3.9	10.5	42.2	75	28	7.0	1.2	0.8	2.4	0.36	410
485819	2.0	2.4	4.9	12	<5	1.5	0.7	<0.5	1.3	0.21	<50
485820	1.5	3.5	11.9	23	10	2.3	0.8	0.6	1.7	0.26	<50
485821	0.8	1.0	4.6	9	6	1.3	0.6	<0.5	0.9	0.15	<50
485822	3.9	76.5	86.6	169	45	9.4	1.0	<0.5	1.2	0.19	260
485823	<0.5	4.2	23.2	52	22	4.9	0.4	<0.5	1.4	0.21	170
485824	<0.5	1.0	15.3	33	13	3.1	0.5	<0.5	1.1	0.16	190
485825	0.8	2.5	27.2	49	18	5.1	1.3	<0.5	0.8	0.13	200
485826	1.2	3.2	12.4	23	7	2.1	1.2	<0.5	1.1	0.16	1700
485827	1.9	3.2	7.7	17	5	2.1	0.5	<0.5	0.7	0.12	310
485828	<0.5	1.5	4.4	9	<5	0.5	0.2	<0.5	0.3	0.05	180
485829	1.8	5.3	17.6	32	10	3.0	1.1	<0.5	1.2	0.19	600
485830	5.3	23.3	26.5	54	16	4.3	1.0	0.9	4.0	0.60	560
485831	5.2	21.9	53.7	109	38	9.0	1.8	1.2	3.2	0.49	685
Samples	152	152	152	152	152	152	152	152	152	152	152
Minimum	<0.5	<0.2	1.0	<3	<5	0.3	<0.2	<0.5	<0.2	<0.05	<75
Maximum	13.3	133.0	179.0	341	131	31.7	6.8	4.3	24.0	3.66	14000
Median	0.8	3.0	17.5	31	12	3.2	0.9	<0.5	1.2	0.20	288

GGU no.	Al pct	Na pct	K pct	Ca pct	P pct	Mg pct	Fe pct	Ti pct	V ppm	Mn ppm
470001	3.96	2.99	2.40	2.20	0.015	0.77	4.37	0.13	41	423
470002	0.80	0.05	0.93	0.21	0.006	0.16	1.98	0.03	7	61
470003	5.40	0.09	0.11	0.40	0.008	2.40	15.50	0.66	344	4885
470004	6.21	1.66	0.49	3.98	0.094	5.35	12.70	0.49	252	1575
470005	13.91	2.81	4.56	3.03	0.028	2.13	6.94	0.70	178	660
470006	5.97	2.77	2.19	2.18	0.005	1.49	8.12	0.95	260	196
470007	13.77	2.61	1.68	1.62	0.012	2.64	9.53	0.60	232	1191
470008	3.68	1.28	0.87	0.89	0.007	1.44	11.60	0.13	116	3281
470009	6.12	1.08	4.11	4.62	0.234	3.66	10.50	3.06	479	1460
470010	2.94	0.40	0.89	3.71	0.037	11.65	11.70	0.45	175	1332
470020	4.17	1.04	0.18	4.50	0.045	1.73	10.40	0.24	92	726
470021	6.28	0.03	0.02	3.46	0.062	1.54	17.30	0.13	47	3692
470022	1.06	0.06	0.02	3.61	0.098	1.28	28.20	0.07	17	1015
470023	5.54	0.73	1.32	4.28	0.126	6.80	13.40	0.58	170	1038
470024	4.71	1.07	1.24	0.44	0.026	1.18	4.58	0.15	56	1258
470025	6.36	0.40	4.85	0.94	0.016	0.67	6.33	0.03	7	111
470026	8.03	0.72	0.95	1.13	0.009	3.17	13.60	0.20	224	1348
470027	2.73	1.26	0.15	0.09	0.005	0.55	6.64	0.13	21	92
470028	2.42	0.14	0.02	7.33	0.019	3.54	5.06	0.13	41	846
470029	5.04	1.90	1.09	8.58	0.046	3.49	8.94	0.47	176	2488
470030	1.50	0.03	1.12	0.58	0.270	0.07	1.83	0.07	11	14
485701	5.33	2.05	1.29	0.78	0.016	1.26	9.87	0.42	286	310
485702	3.88	2.66	0.86	1.93	0.008	0.61	3.48	0.15	47	201
485703	5.18	3.32	4.36	0.75	0.023	0.34	5.75	0.08	37	141
485704	6.86	3.77	1.66	2.83	0.018	0.33	3.45	0.15	16	120
485705	6.61	2.21	0.87	1.76	0.011	1.63	5.44	0.43	112	648
485706	3.98	1.49	1.09	3.05	0.038	2.33	5.63	0.32	133	333
485707	0.02	0.04	0.01	23.23	<0.001	7.42	0.61	<0.01	<2	3669
485708	2.57	0.18	0.07	0.41	0.020	0.82	5.18	0.04	86	1118
485709	1.69	0.01	<0.01	0.33	0.036	1.52	31.80	0.20	24	719
485710	3.95	0.22	0.14	0.40	0.012	2.11	12.60	0.06	41	963
485711	0.26	0.01	0.13	<0.01	0.003	0.01	0.46	0.02	33	23
485712	1.06	0.02	0.55	0.01	0.011	0.06	2.76	0.06	53	25
485713	0.54	0.04	0.42	0.05	0.003	0.03	1.00	0.02	2	7
485714	0.82	0.04	0.73	0.03	0.008	0.07	0.21	0.01	2	6
485715	7.31	0.09	0.01	5.79	0.238	2.45	21.70	3.12	70	3027
485716	0.15	0.07	0.04	<0.01	0.001	0.01	0.42	0.01	9	27
485717	3.07	0.08	1.28	0.07	0.022	1.94	2.54	0.08	23	161
485718	1.88	0.45	1.16	0.08	0.003	0.34	1.15	0.02	7	54
485719	5.31	0.09	2.37	0.11	0.030	1.57	4.40	0.21	66	143
485720	4.48	0.23	1.18	0.09	0.029	0.39	3.67	0.21	93	318
485721	1.72	0.31	0.84	0.07	0.007	0.09	3.16	0.02	5	87

GGU no.	Al pct	Na pct	K pct	Ca pct	P pct	Mg pct	Fe pct	Ti pct	V ppm	Mn ppm
485722	2.66	0.04	0.05	1.61	0.152	1.64	23.10	0.11	42	800
485723	1.23	0.08	0.02	2.55	0.095	0.91	27.80	0.04	20	1677
485724	1.58	0.10	0.07	1.74	0.126	1.10	18.10	0.06	27	422
485725	0.46	0.08	0.10	0.99	0.044	0.76	28.20	0.03	13	316
485726	1.53	0.13	1.56	<0.01	0.004	0.07	0.64	0.04	4	30
485727	0.66	0.20	0.49	2.34	0.012	0.24	3.54	0.03	5	1014
485728	0.61	0.21	0.39	1.98	0.014	0.50	1.65	0.02	5	1469
485729	0.65	0.09	0.02	0.50	0.011	1.97	35.2	0.04	22	25818
485730	0.88	0.08	<0.01	0.67	0.015	0.94	35.60	0.03	26	28051
485731	0.28	0.09	0.01	0.34	0.014	1.18	24.70	0.02	16	14971
485732	1.11	0.08	0.04	0.65	0.072	1.35	29.30	0.08	18	3959
485733	0.65	0.14	0.02	0.40	0.070	1.56	26.40	0.05	15	3484
485734	0.74	0.12	0.01	0.50	0.078	1.59	25.50	0.04	15	4109
485735	4.74	1.37	1.34	5.87	0.032	6.72	13.80	0.99	652	1453
485736	3.04	0.13	1.69	0.78	0.029	0.41	1.76	0.17	53	252
485737	2.60	0.20	1.09	0.14	0.045	0.73	2.09	0.20	35	209
485738	5.04	0.05	3.45	0.19	0.082	0.50	3.49	0.30	69	125
485739	4.41	2.54	1.18	4.53	0.233	1.80	10.10	1.04	243	1516
485740	6.36	2.52	3.17	0.74	0.148	0.95	6.32	0.62	42	619
485741	6.33	0.62	0.30	1.79	0.060	1.70	11.10	0.11	52	822
485742	6.99	1.39	0.47	2.10	0.054	1.87	7.93	0.28	105	689
485743	7.19	0.03	0.21	3.09	0.079	2.27	26.70	0.21	57	2207
485744	4.06	0.02	0.06	1.50	0.090	2.51	22.20	0.28	101	1022
485745	1.60	0.08	0.05	5.51	0.119	1.22	15.20	0.07	28	710
485746	7.95	0.08	0.14	2.28	0.080	2.08	20.60	0.34	83	1300
485747	5.33	0.04	0.08	3.38	0.078	1.30	21.70	0.09	37	561
485748	6.65	1.20	2.72	1.39	0.058	2.18	7.19	0.37	106	723
485749	7.06	2.31	2.46	1.13	0.009	1.34	3.31	0.22	67	490
485750	6.57	2.29	2.50	0.95	0.021	1.58	3.77	0.32	91	418
485751	5.24	0.04	0.03	2.67	0.100	2.12	23.20	0.18	70	1083
485752	2.76	0.02	0.03	1.69	0.063	1.65	20.50	0.12	47	904
485753	6.51	0.05	0.06	2.93	0.077	2.76	26.90	0.17	50	686
485754	4.47	0.05	0.06	3.30	0.078	1.96	19.30	0.18	67	940
485755	10.06	1.37	0.60	3.73	0.237	2.71	10.10	0.70	196	2124
485756	3.83	0.15	0.27	2.47	0.087	0.87	10.40	0.11	28	723
485757	9.42	2.66	3.64	1.79	0.142	1.90	4.61	0.50	100	631
485758	1.57	0.07	0.10	0.44	0.056	0.72	4.52	0.05	18	784
485759	6.45	0.17	1.92	0.08	0.012	0.92	4.12	0.29	69	743
485760	11.27	2.06	0.90	2.45	0.016	1.68	11.40	0.80	164	1431
485761	6.16	0.12	2.18	<0.01	0.003	1.30	3.08	0.41	143	260
485762	4.01	0.08	0.97	0.04	0.020	0.74	14.70	0.19	366	185
485763	1.01	0.13	0.91	<0.01	0.004	0.02	8.99	0.02	3	39
485764	0.70	0.04	0.02	<0.01	<0.001	<0.01	11.00	<0.01	3	24
485765	0.75	0.05	0.05	<0.01	0.001	<0.01	16.60	<0.01	4	20

GGU no.	Al pct	Na pct	K pct	Ca pct	P pct	Mg pct	Fe pct	Ti pct	V ppm	Mn ppm
485766	0.66	0.11	0.03	3.75	0.108	0.74	21.70	0.04	14	865
485767	9.12	1.56	0.99	6.71	0.115	3.55	11.30	1.72	464	1595
485768	4.01	0.47	0.27	5.59	0.354	1.51	16.70	1.70	35	3245
485769	2.56	0.04	0.02	2.58	0.088	1.60	23.40	0.06	30	1957
485770	0.66	0.08	0.03	4.65	0.064	1.12	8.40	0.01	6	936
485771	3.08	<0.01	0.03	2.85	0.081	1.50	21.00	0.12	37	1148
485772	3.31	1.00	4.25	0.17	0.027	0.88	6.50	0.19	207	395
485773	7.33	0.44	1.51	1.09	0.041	4.07	11.40	0.24	69	1131
485774	6.52	1.36	4.17	1.19	0.150	1.66	4.24	0.80	108	411
485775	6.21	0.40	0.64	4.22	0.093	2.90	7.47	1.09	208	1473
485776	7.81	1.48	3.53	6.22	0.246	4.58	8.15	1.75	187	1578
485777	4.28	0.87	5.87	0.18	0.015	0.37	1.79	0.17	52	85
485778	9.53	1.84	5.13	1.63	0.351	3.02	8.82	0.91	225	304
485779	7.47	1.48	2.19	6.98	0.241	4.98	10.40	1.82	229	1449
485780	6.46	0.81	1.61	7.73	0.277	6.67	13.00	0.94	553	1491
485781	7.04	1.01	0.60	1.61	0.021	2.45	10.60	0.09	170	1988
485782	10.29	1.72	2.16	1.27	0.010	2.55	9.02	0.21	179	1080
485783	0.59	0.03	0.17	0.01	0.007	0.17	1.38	0.08	4	116
485784	0.54	0.15	0.03	0.03	0.006	0.27	1.25	0.03	7	41
485785	6.14	2.20	0.53	0.11	0.040	1.29	9.18	0.49	104	227
485786	3.30	0.85	0.16	17.39	0.019	1.96	5.45	0.15	28	1045
485787	6.91	1.23	1.70	7.11	0.014	2.76	6.70	0.29	64	905
485788	5.20	1.47	2.03	0.81	0.349	0.99	9.39	0.48	93	377
485789	2.82	1.43	0.14	0.22	0.005	1.01	3.96	0.1	28	156
485790	2.00	0.18	0.01	20.66	0.026	2.67	5.05	0.07	24	1929
485791	1.54	0.12	1.17	0.26	<0.001	1.10	31.90	<0.01	901	145
485792	6.55	3.11	1.99	4.82	0.040	6.18	4.57	0.46	205	752
485793	5.96	3.28	1.33	5.58	0.034	4.86	6.94	0.39	193	1013
485794	4.54	1.07	2.24	0.30	0.027	2.73	4.48	0.22	91	268
485795	6.10	0.05	1.90	0.11	0.020	5.27	4.30	0.37	127	223
485796	8.06	1.76	3.16	5.17	0.039	5.11	10.60	0.69	381	1560
485797	7.12	0.52	1.64	8.08	0.042	2.15	9.88	0.61	337	4344
485798	3.88	0.98	0.17	11.65	0.030	8.04	6.58	0.11	118	2182
485799	8.51	2.66	1.56	6.41	0.260	3.20	9.73	0.95	295	1206
485800	6.46	1.54	1.94	6.30	0.610	3.84	9.83	1.15	263	1790
485801	6.00	0.49	0.70	5.65	0.026	3.49	19.20	0.55	299	7136
485802	4.32	3.04	2.41	1.88	0.005	0.21	3.45	0.17	25	130
485803	7.16	2.90	0.59	1.27	0.011	2.76	8.08	0.25	60	538
485804	0.20	0.03	0.09	0.01	0.001	0.02	2.27	0.02	2	31
485805	7.83	2.61	1.42	6.02	0.060	3.41	11.60	1.22	253	2042
485806	4.07	1.20	0.59	5.49	0.039	3.38	11.20	0.85	280	2041
485807	4.41	1.26	1.04	8.11	0.056	2.72	11.30	1.01	252	3895
485808	4.64	1.16	1.08	6.94	0.114	2.26	12.60	0.25	83	2619
485809	1.59	0.35	0.46	8.29	0.052	6.08	14.90	0.48	179	3169

GGU no.	Al pct	Na pct	K pct	Ca pct	P pct	Mg pct	Fe pct	Ti pct	V ppm	Mn ppm
485810	3.06	0.45	1.30	4.52	0.072	4.76	20.00	0.58	182	2329
485811	4.92	1.00	2.16	1.14	0.033	2.19	17.50	0.23	84	669
485812	5.94	1.39	2.94	1.02	0.043	2.82	8.90	0.80	137	690
485813	4.40	1.21	2.14	0.73	0.024	2.29	9.46	0.53	76	528
485814	8.89	3.07	2.03	4.91	0.018	4.93	6.24	0.44	164	1002
485815	3.22	0.56	0.69	4.69	0.054	2.18	24.40	0.51	120	1411
485816	5.13	2.16	2.07	1.33	0.011	1.43	15.30	0.24	84	534
485817	7.05	2.37	2.19	4.51	0.229	2.36	15.70	1.30	333	2084
485818	4.11	0.59	2.50	2.61	0.116	2.86	18.10	0.26	82	1235
485819	1.05	0.12	0.27	0.96	0.077	2.18	32.15	0.05	14	1598
485820	1.23	0.22	0.21	1.27	0.106	1.89	28.60	0.10	39	1046
485821	0.44	0.09	0.05	1.71	0.120	1.48	32.00	0.04	29	731
485822	7.00	4.07	1.85	2.35	0.149	0.83	8.33	0.53	115	1112
485823	1.60	0.39	0.21	7.68	0.156	8.71	11.20	0.11	90	3156
485824	4.15	0.74	0.75	11.05	0.009	6.98	14.20	0.24	157	3885
485825	2.14	0.31	0.52	14.53	0.042	5.77	12.30	1.11	212	3390
485826	4.66	1.41	1.96	2.30	0.052	1.88	20.50	0.54	108	5791
485827	4.80	0.49	0.96	2.27	0.056	2.33	14.80	0.20	111	2153
485828	2.11	0.56	0.53	0.45	0.004	0.70	1.99	0.14	43	207
485829	5.21	1.60	1.71	2.10	0.047	1.32	15.10	0.62	133	1263
485830	4.61	0.08	4.33	0.05	0.021	0.47	1.11	0.39	21	64
485831	14.38	0.10	7.44	0.15	0.062	2.53	2.93	0.66	88	189
Samples	152	152	152	152	152	152	151	152	152	152
Minimum	0.02	<0.01	<0.01	<0.01	<0.001	<0.01	0.21	<0.01	<2	6
Maximum	14.38	4.07	7.44	23.23	0.610	11.65	35.60	3.12	901	28051
Median	4.41	0.45	0.88	1.73	0.038	1.65	9.73	0.20	69	885

Table 3. Summary of selected elements for mineralised rock samples from the Qaanaaq region

Geological unit	Sam- ples	Au ppb	Cu ppm	Pb ppm	Zn ppm	Ni ppm	Ti%	Fe%	S%
Quartz veins and basic dykes	6	< 2-5 3	11-1081 119	< 3-13 4	3-104 16	4-63 11	0.02-3.06 0.04	1.2-10.5 3.5	0.03-3.40 0.21
Dundas Group	10	< 2-5 < 2	12-426 57	< 3-157 12	3-20986 76	3-48 26	0.02-0.49 0.13	2.0-9.4 5.5	0.07-4.46 1.82
Baffin Bay Group	10	< 2-7 < 2	7-15247 251	< 3-15 10	4-47 6	1-46 5	0.01-0.39 0.05	0.2-3.0 1.1	0.03-2.20 0.15
Nares Strait Group	5 ¹⁾	< 2-2 < 2	30-10167 920	< 3-12 5	22-60 33	44-119 65	0.22-0.46 0.38	4.3-10.6 4.6	0.01-0.18 0.01
Prudhoe Land supracrustal complex	14	< 2-11 < 2	8-886 40	< 3-135 13	< 1-637 31	< 1-581 26	0.01-3.12 0.09	0.4-21.7 6.3	0.04-18.21 3.17
Undifferentiated gneiss complex	25	< 2-76 < 2	15-1901 354	< 3-171 11	37-1769 98	7-3582 90	0.06-1.82 0.43	1.8-15.5 8.8	0.12-6.05 1.43
Thule mixed- gneiss complex	81	< 2-83 < 2	8-1748 123	< 3-45 < 3	22-793 93	4-3282 50	0.01-1.72 0.24	1.8-35.6 14.8	0.01-10.15 1.11

Numbers are ranges and medians.

Analyses by Activation Laboratories Ltd., Ontario, Canada.

Analytical methods: Inductively coupled plasma emission spectrometry: Cu, Pb, Zn, Ni, Ti, S.

Instrumental neutron activation analysis: Au, Fe.

Fire assay: Au > 50 ppb.

¹⁾ GGU 485791 omitted.

Table 4. *Analytical values from the "Mount Gyrfalco" Showing*

GGU no.	Type	SiO₂ pct	Al₂O₃ pct	Fe₂O₃ pct	MnO pct	MgO pct	CaO pct	Na₂O pct	K₂O pct	TiO₂ pct	P₂O₅ pct	Loi pct	Total pct	S pct	Zn ppm	Au ppb
485729	1.5 m chip	41.21	0.97	49.59	3.145	2.93	0.59	0.02	0.07	0.038	0.03	1.37	99.95	2.53	361	19
485730	2.0 m chip	32.73	1.66	59.72	3.882	3.15	0.86	0.04	<0.01	0.034	0.04	-2.00	100.11	0.32	288	4
485731	3.0 m chip	57.44	0.48	38.23	2.117	1.87	0.42	0.04	0.08	0.027	0.04	-5.00	100.24	0.20	337	6
485732	Grab	50.45	1.82	44.46	0.518	2.50	0.81	0.06	0.05	0.077	0.19	-1.02	99.92	0.08	90	<2
485733	Grab	55.47	1.13	41.19	0.443	2.45	0.49	0.08	0.04	0.061	0.18	-1.88	99.65	0.07	114	<2
485734	Grab	54.90	1.34	41.51	0.533	2.72	0.62	0.06	<0.01	0.057	0.20	-1.72	100.22	0.04	111	<2

Analysis by Activation Laboratories Ltd., Ontario, Canada.
Analytical methodes: XRF, except S and Zn: ICP and Au: FA/ICP.
Negative Loi represent a gain on ignition.